

1 **OGT binds a conserved C-terminal domain of TET1 to regulate TET1 activity and function in**  
2 **development**

3

4 Joel Hrit<sup>1,2</sup>, Cheng Li<sup>3,4</sup>, Elizabeth Allene Martin<sup>1,2</sup>, Mary Goll<sup>3</sup>, and Barbara Panning<sup>1\*</sup>

5

6 <sup>1</sup>Department of Biochemistry and Biophysics, University of California San Francisco, San  
7 Francisco, CA, United States

8 <sup>2</sup>TETRAD Graduate Program, University of California San Francisco, San Francisco, CA, United  
9 States

10 <sup>3</sup>Developmental Biology Program, Memorial Sloan Kettering Cancer Center, New York, NY, USA

11 <sup>4</sup>Program in Biochemistry and Structural Biology, Cell and Developmental Biology, and  
12 Molecular Biology, Weill Cornell Graduate School of Medical Sciences, Cornell University, New  
13 York, NY, USA

14 \*Correspondence: [barbara.panning@ucsf.edu](mailto:barbara.panning@ucsf.edu)

15

16

17

18

19

20

21

22

23

24

25

26

27

28

29

30

31

32

33

34

35

36

37

38

39

40

41

42

43

44

## 45 **Abstract**

46 Mammalian TET enzymes oxidize 5-methylcytosine to 5-hydroxymethylcytosine and  
47 higher oxidized derivatives. TETs are targets of the enzyme OGT, which post-translationally  
48 modifies intracellular proteins in response to cellular nutrient status. The biological implications  
49 of the OGT-TET interaction have not been thoroughly explored. Here, we show for the first time  
50 that modification of TET1 by OGT enhances its activity *in vitro*. We identify a previously  
51 uncharacterized domain of TET1 responsible for binding to OGT and report a point mutation  
52 that disrupts the OGT-TET1 interaction. Finally, we show that the interaction between TET1 and  
53 OGT is necessary for TET1 to rescue *tet* mutant zebrafish hematopoietic stem cell formation,  
54 suggesting that OGT promotes TET1's function in development. Our results demonstrate  
55 regulation of TET activity by OGT *in vitro* and *in vivo*. These results link metabolism and  
56 epigenetic control, which may be relevant to the developmental and disease processes  
57 regulated by these two enzymes.  
58  
59

## 60 **Introduction**

61 Methylation at the 5' position of cytosine in DNA is a widespread epigenetic regulator of  
62 gene expression. Proper deposition and removal of this mark is indispensable for normal  
63 vertebrate development, and misregulation of DNA methylation is a common feature in many  
64 diseases [1,2]. The discovery of the Ten-Eleven Translocation (TET) family of enzymes, which  
65 iteratively oxidize 5-methylcytosine (5mC) to 5-hydroxymethylcytosine (5hmC), 5-  
66 formylcytosine (5fC), and 5-carboxylcytosine (5caC), has expanded the epigenome [3-7]. These  
67 modified cytosines have multiple roles, functioning both as transient intermediates in an active  
68 DNA demethylation pathway [6,8-11] and as stable epigenetic marks [12,13] that may recruit  
69 specific readers [14].

70 One interesting interaction partner of TET proteins is *O*-linked N-acetylglucosamine (*O*-  
71 GlcNAc) Transferase (OGT). OGT is the sole enzyme responsible for attaching a GlcNAc sugar to  
72 serine and threonine residues of over 1,000 nuclear, cytoplasmic, and mitochondrial proteins  
73 [15,16]. Like phosphorylation, *O*-GlcNAcylation is a reversible modification that affects the  
74 function of target proteins. OGT's targets regulate gene expression [17,18], metabolism  
75 [16,19,20], and signaling [21,22], consistent with OGT's role in development and disease  
76 [23,24].

77 OGT stably interacts with and modifies all three TET proteins and its genome-wide  
78 distribution overlaps significantly with TETs [25-27]. Two studies in mouse embryonic stem cells  
79 (mESCs) have suggested that TET1 and OGT may be intimately linked in regulation of gene  
80 expression, as depleting either enzyme reduced the chromatin association of the other and  
81 affected expression of its target genes [25,28]. However, it is unclear to what extent these  
82 genome-wide changes are direct effects of perturbing the TET1-OGT interaction. Further work  
83 is necessary to uncover the biological importance of the partnership between TET1 and OGT.

84 In this work, we map the interaction between TET1 and OGT to a small C-terminal region  
85 of TET1, that is both necessary and sufficient to bind OGT. We show for the first time that OGT  
86 modifies the catalytic domain of TET1 *in vitro* and enhances its catalytic activity. Finally, we  
87 show that OGT levels correlate with TET activity in mESCs and use mutant TET1 to show that  
88 the TET1-OGT interaction promotes Tet1 function in the developing zebrafish embryo. Together

89 these results suggest that OGT regulates TET1 activity, indicating that the TET1-OGT interaction  
90 may be two-fold in function – allowing TET1 to recruit OGT to specific genomic loci and allowing  
91 OGT to modulate TET1 activity.

92  
93

## 94 **Materials and Methods**

95  
96

### 96 **Cell Culture**

97 The mESC line LF2, and its derivatives, and a line expressing transgenic BirA-tag OGT [25]  
98 were routinely passaged by standard methods in KO-DMEM, 10% FBS, 2 mM glutamine, 1X non-  
99 essential amino acids, 0.1 mM β-mercaptoethanol and recombinant leukemia inhibitory factor.  
100 HEK293T were cultured in DMEM, 10% FBS, and 2 mM glutamine.

101  
102

### 102 **Recombinant protein purification**

103 Full-length human OGT in the pBJG vector was transformed into BL-21 DE3 E. coli. A  
104 liquid culture was grown in LB + 50µg/mL kanamycin at 37C until OD<sub>600</sub> reached 1.0. IPTG was  
105 added to 1mM final and the culture was induced at 16C overnight. Cells were pelleted by  
106 centrifugation and resuspended in 5mL BugBuster (Novagen) + protease inhibitors (Sigma  
107 Aldrich) per gram of cell pellet. Cells were lysed on an orbital shaker for 20 minutes at room  
108 temperature. The lysate was clarified by centrifugation at 30,000g for 30 minutes at 4C.  
109 Clarified lysate was bound to Ni-NTA resin (Qiagen) at 4C and then poured over a disposable  
110 column. The column was washed with 6 column volumes of wash buffer 1 (20mM Tris pH 8,  
111 1mM CHAPS, 10% glycerol, 5mM BME, 10mM imidazole, 250mM NaCl) followed by 6 column  
112 volumes of wash buffer 2 (wash buffer 1 with 50mM imidazole). The protein was eluted in 4  
113 column volumes of elution buffer (20mM Tris pH 8, 1mM CHAPS, 5mM BME, 250mM imidazole,  
114 250mM NaCl). Positive fractions were pooled and dialyzed into storage buffer (20mM Tris pH 8,  
115 1mM CHAPS, 0.5mM TCEP, 10% glycerol, 150mM NaCl, 1mM EDTA), flash frozen in liquid  
116 nitrogen and stored at -80C in small aliquots.

117 Mouse TET1 catalytic domain (aa1367-2039) was expressed in sf9 insect cells according  
118 to the Bac-to-Bac Baculovirus Expression System. Constructs were cloned into the pFastBac HTA  
119 vector and transformed in DH10Bac E. coli for recombination into a bacmid. Bacmid containing  
120 the insert was isolated and used to transfect adherent sf9 cells for 6 days at 25C. Cell media (P1  
121 virus) was isolated and used to infect 20mL of sf9 cells in suspension for 3 days. Cell media (P2  
122 virus) was isolated and used to infect a larger sf9 suspension culture for 3 days. Cells were  
123 pelleted by centrifugation, resuspended in lysis buffer (20mM Tris pH 8, 1% Triton, 10%  
124 glycerol, 20mM imidazole, 50mM NaCl, 1mM MgCl<sub>2</sub>, 0.5mM TCEP, protease inhibitors, 2.5U/mL  
125 benzonase), and lysed by douncing and agitation at 4C for 1 hour. The lysate was clarified by  
126 centrifugation at 48,000g for 30 minutes at 4C and bound to Ni-NTA resin (Qiagen) at 4C, then  
127 poured over a disposable column. The column was washed with 5 column volumes of wash  
128 buffer (20mM Tris pH 8, 0.3% Triton, 10% glycerol, 20mM imidazole, 250mM NaCl, 0.5mM  
129 TCEP, protease inhibitors). The protein was eluted in 5 column volumes of elution buffer  
130 (20mM Tris pH 8, 250mM imidazole, 250mM NaCl, 0.5mM TCEP, protease inhibitors). Positive  
131 fractions were pooled and dialyzed overnight into storage buffer (20mM Tris pH 8, 150mM  
132 NaCl, 0.5mM TCEP). Dialyzed protein was purified by size exclusion chromatography on a

133 120mL Superdex 200 column (GE Healthcare). Positive fractions were pooled, concentrated,  
134 flash frozen in liquid nitrogen and stored at -80C in small aliquots.

135

### 136 **Overexpression in HEK293T cells and immunoprecipitation**

137 Mouse Tet1 catalytic domain (aa1367-2039) and truncations and mutations thereof  
138 were cloned into the pcDNA3b vector. GFP fusion constructs were cloned into the pcDNA3.1  
139 vector. Human OGT constructs were cloned into the pcDNA4 vector. Plasmids were transiently  
140 transfected into adherent HEK293T cells at 70-90% confluency using the Lipofectamine 2000  
141 transfection reagent (ThermoFisher) for 1-3 days.

142 Full-length mouse Tet1 and mutations thereof were cloned into the pCAG vector.  
143 Plasmids were transiently transfected into adherent HEK293T cells at 70-90% confluency using  
144 the PolyJet transfection reagent (SignaGen) for 1-3 days.

145 Transiently transfected HEK293T cells were harvested, pelleted, and lysed in IP lysis  
146 buffer (50mM Tris pH 8, 200mM NaCl, 1% NP40, 1x HALT protease/phosphatase inhibitors). For  
147 pulldown of FLAG-tagged constructs, cell lysate was bound to anti-FLAG M2 magnetic beads  
148 (Sigma Aldrich) at 4C. For pulldown of GFP constructs, cell lysate was bound to magnetic  
149 protein G dynabeads (ThermoFisher) conjugated to the JL8 GFP monoclonal antibody (Clontech)  
150 at 4C. Beads were washed 3 times with IP wash buffer (50mM Tris pH 8, 200mM NaCl, 0.2%  
151 NP40, 1x HALT protease/phosphatase inhibitors). Bound proteins were eluted by boiling in SDS  
152 sample buffer.

153

### 154 ***In vitro* transcription/translation and immunoprecipitation**

155 GFP fused to TET C-terminus peptides were cloned into the pcDNA3.1 vector and  
156 transcribed and translated *in vitro* using the TNT Quick Coupled Transcription/Translation  
157 System (Promega).

158 For immunoprecipitation, recombinant His-tagged OGT was coupled to His-Tag isolation  
159 dynabeads (ThermoFisher). Beads were bound to *in vitro* translation extract diluted 1:1 in  
160 binding buffer (40mM Tris pH 8, 200mM NaCl, 40mM imidazole, 0.1% NP40) at 4C. Beads were  
161 washed 3 times with wash buffer (20mM Tris pH 8, 150mM NaCl, 20mM imidazole, 0.1% NP40).  
162 Bound proteins were eluted by boiling in SDS sample buffer.

163

### 164 **Recombinant protein binding assay**

165 20uL reactions containing 2.5uM rOGT and 2.5uM rTET1 CD wt or D2018A were  
166 assembled in binding buffer (50mM Tris pH 7.5, 100mM NaCl, 0.02% Tween-20) and pre-  
167 incubated at room temperature for 15 minutes. TET1 antibody (Millipore 09-872) was bound to  
168 magnetic Protein G Dynabeads (Invitrogen), and beads added to reactions following pre-  
169 incubation. Reactions were bound to beads for 10 minutes at room temperature. Beads were  
170 washed 3 times with 100uL binding buffer, and bound proteins were recovered by boiling in  
171 SDS sample buffer and analyzed by SDS-PAGE and coomassie stain.

172

### 173 **Western blots**

174 For western blot, proteins were separated on a denaturing SDS-PAGE gel and  
175 transferred to PVDF membrane. Membranes were blocked in PBST + 5% nonfat dry milk at  
176 room temp for >10 minutes or at 4C overnight. Primary antibodies used for western blot were:

177 FLAG M2 monoclonal antibody (Sigma Aldrich F1804), OGT polyclonal antibody (Santa Cruz  
178 sc32921), OGT monoclonal antibody (Cell Signaling D1D8Q), His6 monoclonal antibody (Thermo  
179 MA1-21315), and JL8 GFP monoclonal antibody (Clontech). Secondary antibodies used were  
180 goat anti-mouse HRP and goat anti-rabbit HRP from BioRad. Blots were incubated with Pico  
181 Chemiluminescent Substrate (ThermoFisher) and exposed to film in a dark room.

182

### 183 **Slot blot**

184 Prior to dilution of genomic DNA samples, biotinylated *E. coli* gDNA was added as a  
185 loading control (see below). DNA samples were denatured in 400mM NaOH + 10mM EDTA by  
186 heating to 95C for 10 minutes. Samples were placed on ice and neutralized by addition of 1  
187 volume of cold NH<sub>4</sub>OAc pH 7.2. DNA was loaded onto a Hybond N+ nylon membrane (GE) by  
188 vacuum using a slot blot apparatus. The membrane was dried at 37C and DNA was covalently  
189 linked to the membrane by UV crosslinking (700uJ/cm<sup>2</sup> for 3 minutes). Antibody binding and  
190 signal detection were performed as outlined for western blotting. Primary antibodies used were  
191 5mC monoclonal antibody (Active Motif 39649) and 5hmC monoclonal antibody (Active Motif  
192 39791).

193 For the loading control, membranes were analyzed using the Biotin Chromogenic  
194 Detection Kit (Thermo Scientific) according to the protocol. Briefly, membranes were blocked,  
195 probed with streptavidin conjugated to alkaline phosphatase (AP), and incubated in the AP  
196 substrate BCIP-T (5-bromo-4-chloro-3-indolyl phosphate, p-toluidine salt). Cleavage of BCIP-T  
197 causes formation of a blue precipitate.

198

### 199 **Preparation of lambda DNA substrate**

200 Linear genomic DNA from phage lambda (dam-, dcm-) containing 12bp 5' overhangs was  
201 purchased from Thermo Scientific. Biotinylation was performed by annealing and ligating a  
202 complementary biotinylated DNA oligo. Reactions containing 175ng/uL lambda DNA, 2uM  
203 biotinylated oligo, and 10mM ATP were assembled in 1x T4 DNA ligase buffer, heated to 65C,  
204 and cooled slowly to room temperature to anneal. 10uL T4 DNA ligase was added and ligation  
205 was performed overnight at room temperature. Biotinylated lambda DNA was purified by PEG  
206 precipitation. To a 500uL ligation reaction, 250uL of PEG8000 + 10mM MgCl<sub>2</sub> was added and  
207 reaction was incubated at 4C overnight with rotation. The next day DNA was pelleted by  
208 centrifugation at 14,000g at 4C for 5 minutes. Pellet was washed with 1mL of 75% ethanol and  
209 resuspended in TE.

210 Biotinylated lambda DNA was methylated using M.SssI CpG methyltransferase from  
211 NEB. 20uL reactions containing 500ng lambda DNA, 640uM S-adenosylmethionine, and 4 units  
212 methyltransferase were assembled in 1x NEBuffer 2 supplemented with 20mM Tris pH 8 and  
213 incubated at 37C for 1 hour. Complete methylation was confirmed by digestion with the  
214 methylation-sensitive restriction enzyme BstUI from NEB.

215

### 216 ***In vitro* TET1 CD O-GlcNAcylation**

217 *In vitro* modification of rTET1 CD with rOGT was performed as follows: 10uL reactions  
218 containing 1uM rTET1 CD, 10uM rOGT, and 2.5mM UDP-GlcNAc were assembled in reaction  
219 buffer (50mM Tris pH 7.5, 12.5mM MgCl<sub>2</sub>, 2% glycerol, 1mM DTT) and incubated at 37C for 30-  
220 60 minutes.

221

### 222 ***In vitro* TET1 CD activity assays**

223 20uL reactions containing 100ng biotinylated, methylated lambda DNA, rTET1 CD (from  
224 frozen aliquots or from *in vitro* O-GlcNAcylation reactions), and TET cofactors (1mM alpha-  
225 ketoglutarate, 2mM ascorbic acid, 100uM ferrous ammonium sulfate) were assembled in  
226 reaction buffer (50mM HEPES pH 6.5, 100mM NaCl) and incubated at 37C for 1 hour. Reactions  
227 were stopped by incubation at 65C for 5 minutes, then cooled slowly to room temperature to  
228 allow re-annealing of DNA. DNA was digested to fragments <10kb and purified using DNA clean  
229 and concentrator kit (Zymo). 5hmC content was analyzed by slot blot.

230

### 231 **Generation of mouse embryonic stem cell lines**

232 mESC lines (Fig. S4A, B) were derived using CRISPR-Cas9 genome editing. A guide RNA to  
233 the Tet1 3'UTR was cloned into the px459-Cas9-2A-Puro plasmid using published protocols [29]  
234 with minor modifications. Templates for homology directed repair were amplified from Gene  
235 Blocks (IDT) (Tables S1 and S2). Plasmid and template were co-transfected into LF2 mESCs using  
236 FuGENE HD (Promega) according to manufacturer protocol. After two days cells were selected  
237 with puromycin for 48 hours, then allowed to grow in antibiotic-free media. Cells were  
238 monitored for green or red fluorescence (indicating homology directed repair) and fluorescent  
239 cells were isolated by FACS 1-2 weeks after transfection. All cell lines were propagated from  
240 single cells and correct insertion was confirmed by PCR genotyping (Fig. S4A, B, Table S1).

241

### 242 **Immunofluorescence**

243 For IF experiments, cells were cytopun onto glass slides at 800rpm for 3 minutes. For  
244 5mC or 5hmC staining alone, cells were fixed in 3:1 methanol:acetic acid for 5 minutes. For co-  
245 staining for 5hmC and FLAG, cells were fixed in 4% paraformaldehyde for 10 minutes. Fixed  
246 slides were washed with PBS + 0.01% Tween-20 (PBST) and stored in 70% ethanol at -20C until  
247 use.

248 Fixed slides were incubated in 1M HCl at 37C for 45 minutes to denature chromatin,  
249 then neutralized in 100mM Tris pH 7.6 at room temperature for 10 minutes. Slides were  
250 washed twice in PBST for 5 minutes, then blocked in IF blocking buffer (PBS + 5% goat serum,  
251 0.2% fish skin gelatin, 0.2% Tween-20) at room temperature for 1 hour. Primary antibodies  
252 were diluted in blocking buffer and incubated on slides at 4C overnight. Primary antibodies  
253 used were FLAG M2 monoclonal antibody (Sigma Aldrich F1804), 5mC monoclonal antibody  
254 (Active Motif 39649), and 5hmC polyclonal antibody (Active Motif 39791). Slides were washed  
255 twice in PBST for 5 minutes, then incubated with secondary antibodies diluted in IF blocking  
256 buffer. Secondary antibodies used were Alexa488-conjugated goat anti-rabbit IgG (Jackson 711-  
257 545-152), Cy3-conjugated goat anti-rabbit IgG (Jackson 715-165-152), and Cy3-conjugated goat  
258 anti-mouse IgG (Jackson 715-165-150). Slides were washed three times in PBST for 5 minutes  
259 with DAPI added to the second wash (final concentration 100ng/mL). Slides were then mounted  
260 using prolong gold antifade (Molecular Probes P36930) and imaged.

261

### 262 **mRNA rescue experiments**

263 Zebrafish husbandry was conducted under full animal use and care guidelines with  
264 approval by the Memorial Sloan-Kettering animal care and use committee. For mRNA rescue

265 experiments, mTET1D2018A and mTET1wt plasmids were linearized by NotI digestion. Capped  
266 RNA was synthesized using mMessage mMachine (Ambion) with T7 RNA polymerase. RNA was  
267 injected into one-cell-stage embryos derived from  $tet2^{mk17/mk17}$ ,  $tet3^{mk18/+}$  intercrosses at the  
268 concentration of 100pg/embryo [30]. Injected embryos were raised under standard conditions  
269 at 28.5°C until 30 hours post-fertilization (hpf) at which point they were fixed for *in situ*  
270 hybridization using an antisense probe for *runx1*. The *runx1* probe is described in [31]; *in situ*  
271 hybridization was performed using standard methods [32]. *tet2/3* double mutants were  
272 identified based on morphological criteria and mutants were confirmed by PCR genotyping after  
273 *in situ* hybridization using previously described primers [30].

274 For sample size estimation for rescue experiments, we assume a background mean of  
275 20% positive animals in control groups. We anticipate a significant change would result in at  
276 least a 30% difference between the experimental and control means with a standard deviation  
277 of no more than 10. Using the 1-Sample Z-test method, for a specified power of 95% the  
278 minimum sample size is 4. Typically, zebrafish crosses generate far more embryos than  
279 required. Experiments are conducted using all available embryos. The experiment is discarded if  
280 numbers for any sample are below this minimum threshold when embryos are genotyped at  
281 the end of the experimental period. Results from five independent experiments were reported;  
282 p values were derived from the unpaired two-tailed *t* test.

283 For the dot blot, genomic DNA was isolated from larvae at 30hpf by phenol-chloroform  
284 extraction and ethanol precipitation. Following RNase treatment and denaturation, 2-fold  
285 serially diluted DNA was spotted onto nitrocellulose membranes. Cross-linked membranes were  
286 incubated with 0.02% methylene blue to validate uniform DNA loading. Membranes were  
287 blocked with 5% BSA and incubated with anti-5hmC antibody (1:10,000; Active Motif) followed  
288 by a horseradish peroxidase-conjugated antibody (1:15,000; Active Motif). Signal was detected  
289 using the ECL Prime Detection Kit (GE).

290

### 291 **Reproducibility and Rigor**

292 All immunostaining, IP-Westerns, and genomic DNA slot blot data are representative of  
293 at least three independent biological replicates (experiments carried out on different days with  
294 a different batch of HEK293T cells or mESCs). For targeted mESC lines, three independently  
295 derived lines for each genotype were assayed in at least two biological replicates. For *in vitro*  
296 activity and binding assays using recombinant proteins (representing multiple protein  
297 preparations), data represent at least three technical replicates (carried out on multiple days).  
298 The zebrafish rescue experiment was performed five times (biological replicates), with dot blots  
299 carried out three times. We define an outlier as a result in which all the controls gave the  
300 expected outcome but the experimental sample yielded an outcome different from other  
301 biological or technical replicates. There were no outliers or exclusions.

302

303

## 304 **Results**

305

### 306 **OGT enhances TET activity *in vitro* and in cells**

307 TETs have been implicated in localizing OGT to chromatin, however a role for OGT in  
308 regulation of TETs has not been fully explored. To examine whether OGT can regulate activity of

309 a TET protein, we employed recombinant enzymes to assess the effects of OGT on TET1 activity.  
310 We purified recombinant mouse TET1 catalytic domain (rTET1 CD, aa1367-2039) from sf9 cells  
311 and recombinant human OGT (rOGT; identical to mouse at 1042 of 1046 residues) from *E. coli*  
312 (Fig. S1). rTET1 CD catalyzed formation of 5hmC on an *in vitro* methylated lambda DNA  
313 substrate, dependent on the presence of the TET cofactors alpha-ketoglutarate, Fe<sup>2+</sup>, and  
314 ascorbic acid (Fig. S2). Incubation of rTET1 CD with rOGT and OGT's cofactor UDP-GlcNAc  
315 resulted in O-GlcNAcylation of rTET1 CD (Fig. 1A). Modified rTET1 CD produced more 5hmC  
316 than unmodified rTET1 CD (Fig. 1B, C), indicating that OGT stimulates the activity of the TET1 CD  
317 *in vitro*.

318 To examine whether OGT affects TET activity in a more biological context, we assessed  
319 the effects of altering OGT levels in mESCs. These cells express TET1 and TET2 [33] and the  
320 proteins that remove 5fC and 5caC and replace them with unmodified cytosine. Thus increased  
321 TET activity should manifest as decreased 5mC and 5hmC. We examined levels of 5mC and  
322 5hmC in mESCs overexpressing OGT (Fig. 1D) by immunofluorescence (Fig. 1E) and by slot blot  
323 of genomic DNA (Fig. 1F). These experiments clearly show that overexpression of OGT reduces  
324 the levels of both 5mC and 5hmC, consistent with increased TET activity oxidizing 5hmC to 5fC  
325 and 5caC. These results are consistent with OGT stimulation of TET activity in mESCs.

326

### 327 **A short C-terminal region of TET1 is necessary for binding to OGT**

328 To examine whether OGT regulates TET1 activity *in vivo*, it is necessary to specifically  
329 disrupt the TET1-OGT interaction. All three TETs interact with OGT via their catalytic domains  
330 [26,27,34]. We sought to identify the domain within the TET1 CD responsible for binding to  
331 OGT. The TET1 CD consists of a cysteine rich N-terminal region necessary for co-factor and  
332 substrate binding, a catalytic fold consisting of two lobes separated by a spacer of unknown  
333 function, and a short C-terminal region also of unknown function (Fig. 2A). We transiently  
334 transfected HEK293T cells with FLAG-tagged mouse TET1 CD constructs bearing deletions of  
335 each of these regions, some of which failed to express (Fig. 2B). Because HEK293T cells have  
336 low levels of endogenous OGT, we also co-expressed myc-tagged human OGT. TET1 constructs  
337 were immunoprecipitated (IPed) using FLAG antibody and analyzed for interaction with OGT.  
338 We found that deletion of only the 45 residue C-terminus of TET1 (hereafter TET1 C45)  
339 prevented detectable interaction with OGT (Fig. 2C, TET1 CD del. 4). To exclude the possibility  
340 that this result is an artifact of OGT overexpression, we repeated the experiment  
341 overexpressing only TET1. TET1 CD, but not TET1 CD ΔC45, interacted with endogenous OGT,  
342 confirming that the C45 is necessary for this interaction (Fig. S3).

343 OGT has two major domains: the N-terminus consists of 13.5 tetratricopeptide repeat  
344 (TPR) protein-protein interaction domains, and the C-terminus contains the bilobed catalytic  
345 domain (Fig. 2D). We made internal deletions of several sets of TPRs to ask which are  
346 responsible for binding to the TET1 CD. We co-transfected HEK293T cells with FLAG-TET1 CD  
347 and His6-tagged OGT constructs and performed FLAG IP and western blot as above. We found  
348 that all the TPR deletions tested impaired the interaction with TET1 CD, with deletion of TPRs 7-  
349 9, 10-12, or 13-13.5 being most severe (Fig. 2E). This result suggests that all of OGT's TPRs may  
350 be involved in binding to the TET1 CD, or that deletion of a set of TPRs disrupts the overall  
351 structure of the repeats in a way that disfavors binding.

352



### 353 **Conserved residues in the TET1 C45 are necessary for the TET1-OGT interaction**

354 An alignment of the TET1 C45 region with the C-termini of TET2 and TET3 revealed  
355 several conserved residues (Fig. 3A). We mutated clusters of three conserved residues in the  
356 TET1 C45 of FLAG-tagged TET1 CD (Fig. 3B) and co-expressed these constructs with myc-OGT in  
357 HEK293T cells. FLAG pulldowns revealed that two sets of point mutations disrupted the  
358 interaction with OGT: mutation of D2018, V2021, and T2022, or mutation of V2021, T2022, and  
359 S2024 (Fig. 3C, mt1 and mt2). These results suggested that the residues between D2018 and  
360 S2024 are crucial for the interaction between TET1 and OGT. We mutated these residues  
361 individually and found that D2018A eliminated detectable interaction between FLAG-tagged  
362 TET1 CD and myc-OGT (Fig. 3D).

363 To examine whether D2018 was necessary for the TET1-OGT interaction in the context  
364 of full length TET1, we generated a D2018A mutation in both copies of the *Tet1* gene in mESCs  
365 (Fig. S4A, B). A FLAG tag was also introduced onto the C-terminus of wild type or D2018A  
366 mutant TET1. FLAG pulldowns revealed that the D2018A mutation reduced, but did not  
367 eliminate, co-IP of OGT with TET1 (Fig. 3E). This reduction of OGT was consistent in multiple  
368 experiments and across multiple independently derived cell lines (Fig. S4C). In mESCs, TET1 and  
369 OGT are found together in high molecular weight complexes [25] and interactions of TET1 and  
370 OGT with other proteins in these complexes may be sufficient to support some TET1-OGT  
371 interaction when D2018 is mutated (see discussion).

372

### 373 **The TET1 C-terminus is sufficient for binding to OGT**

374 Having shown that the TET1 C45 is necessary for the interaction with OGT, we next  
375 examined if it is also sufficient to bind OGT. We fused the TET1 C45 to the C-terminus of GFP  
376 (Fig. 4A) and investigated its interaction with OGT. We transiently transfected GFP or GFP-TET1  
377 C45 into HEK293T cells and pulled down with a GFP antibody. We found that GFP-TET1 C45, but  
378 not GFP alone, bound OGT (Fig. 4B), indicating that the TET1 C45 is sufficient for interaction  
379 with OGT.

380 To determine if the interaction between TET1 CD and OGT is direct, we employed  
381 recombinant proteins in pulldown assays using beads conjugated to a TET1 antibody. We found  
382 that wild-type rTET1 CD, but not beads alone, pulled down OGT, indicating a direct interaction  
383 between these proteins (Fig. 4C). rTET1 CD D2018A did not pull down rOGT, consistent with our  
384 mutational analysis in cells. Then we used an *in vitro* transcription/translation extract to  
385 produce GFP and GFP-TET1 C45, incubated each with rOGT, and found that the TET1 C45 is  
386 sufficient to confer binding to rOGT (Fig. 4D). The D2018A mutation was also sufficient in this  
387 context to prevent OGT binding (Fig. 4D), consistent with the behavior of this mutant in cells.  
388 Together these results indicate that the TET1-OGT interaction is direct and mediated by the  
389 TET1 C45.

390

### 391 **TET1 D2018A is active in HEK293T cells**

392 The D2018A mutation lies outside the catalytic fold, suggesting that this mutation is  
393 unlikely to affect TET1 activity. Consistent with this suggestion, in human TET2 the region  
394 homologous to TET1 C45 is dispensable for catalytic activity *in vitro* [35]. To test whether full  
395 length TET1 D2018A is catalytically active, we examined its activity in cells. FLAG-tagged full-  
396 length wild type or D2018A TET1 were transfected into HEK293T cells, which express low levels

397 of OGT and of all three TETs, facilitating a more direct comparison of the two TET1 constructs.  
398 Western blot confirmed that the two proteins were expressed at comparable levels (Fig. 5A).  
399 Immunostaining for FLAG and 5hmC showed that wild type and D2018A TET1 both exhibited  
400 nuclear localization (Fig. 5B). While mock transfected HEK293T cells showed very low levels of  
401 5hmC, consistent with their low expression of TETs and OGT, wild type or D2018A TET1 each  
402 caused increased production of 5hmC (Fig. 5B). A slot blot assay on genomic DNA from these  
403 cells confirmed that comparable levels of 5hmC were observed in wild type and D2018A TET1  
404 transfections (Fig. 5C). These results indicate that the D2018A mutation does not notably impair  
405 TET1's catalytic activity.

406

### 407 **The TET-OGT interaction promotes Tet1 function in the zebrafish embryo**

408 We used zebrafish as a model system to ask whether the D2018A mutation affects TET  
409 function during development. Deletion analysis of *tets* in zebrafish showed that Tet2 and Tet3  
410 are the most important in development, while Tet1 contribution is relatively limited [30].  
411 Deletion of both *tet2* and *tet3* (*tet2/3<sup>DM</sup>*) causes a severe decrease in 5hmC levels accompanied  
412 by larval stage lethality owing to a number of abnormalities including defects in hematopoietic  
413 stem cell (HSC) production. A critical transcription factor, Runx1, marks HSCs in the dorsal aorta  
414 of wild-type embryos, but is largely absent in this region of *tet2/3<sup>DM</sup>* embryos. 5hmC levels and  
415 *runx1* expression are rescued by injection of human TET2 or TET3 mRNA into one-cell-stage  
416 embryos [30].

417 Given strong sequence conservation among vertebrate TET/Tet proteins, we asked if  
418 over expression of Tet1 mRNA could also rescue HSCs in *tet2/3<sup>DM</sup>* zebrafish embryos and if this  
419 rescue is OGT interaction-dependent. To this end, *tet2/3<sup>DM</sup>* embryos were injected with wild  
420 type or D2018A mutant encoding Tet1 mRNA at the one cell stage. At 30 hours post  
421 fertilization (hpf) embryos were fixed and the presence of *runx1* positive HSCs in the dorsal  
422 aorta was assessed by *in situ* hybridization (Fig. 6A). Tet1 wild type mRNA significantly  
423 increased the percentage of embryos with high *runx1*, while Tet1 D2018A mRNA failed to  
424 rescue *runx1* positive cells (Fig. 6A-B). We also performed dot blots with genomic DNA from  
425 these embryos to measure levels of 5hmC (Fig. 6C). Embryos injected with wild type Tet1 mRNA  
426 showed a modest increase in 5hmC relative to uninjected *tet2/3<sup>DM</sup>* embryos, while injection of  
427 TET1 D2018A mRNA did not show an increase. These results suggest that the OGT-TET1  
428 interaction promotes both TET1's catalytic activity and its ability to rescue *runx1* expression in  
429 this system.

430

431

## 432 **Discussion**

433

### 434 **OGT stimulation of TET activity**

435 Our results show for the first time that OGT stimulates the activity of a TET protein *in*  
436 *vitro*. The mechanism underlying this stimulation is unclear; it may be the result of the protein-  
437 protein interaction, the O-GlcNAc modification, or both. Further experiments uncoupling these  
438 elements will be informative.

439 Our data demonstrate that OGT stimulates TET1 activity *in vitro* and are consistent with  
440 a role for OGT in TET1 regulation *ex vivo* and *in vivo*. OGT also directly interacts with TET2 and

441 TET3, suggesting that it may regulate all three TET proteins. Notably, although all three TETs  
442 possess highly similar catalytic folds and the same catalytic activity *in vitro*, they show a number  
443 of differences that are likely to determine their biological role. Different TET proteins are  
444 expressed in different cell types and at different stages of development [36-39]. TET1 and TET2  
445 appear to target different genomic regions [40] and to promote different pluripotent states in  
446 mESCs [41]. The mechanisms responsible for these differences are not well understood. We  
447 suggest that OGT is a strong candidate for regulation of TET enzymes.

448

#### 449 **A unique OGT interaction domain?**

450 We identified a 45-amino acid domain of TET1 that is both necessary and sufficient for  
451 binding of OGT. To our knowledge, this is the first time that a small protein domain has been  
452 identified that confers stable binding to OGT. The vast majority of OGT targets do not bind to  
453 OGT tightly enough to be detected in co-IP experiments, suggesting that OGT's interaction with  
454 TET proteins is unusually strong. For determination of the crystal structure of the human TET2  
455 catalytic domain in complex with DNA, the corresponding C-terminal region had to be deleted  
456 [35], suggesting that it may be unstructured. When bound to OGT this domain may become  
457 structured, and structural studies of OGT bound to C45 could shed light on what features make  
458 this domain uniquely able to interact stably with OGT and how OGT may stimulate TET1  
459 activity.

460 An alternative or additional role for the stable TET-OGT interaction may be recruitment  
461 of OGT to chromatin by TET proteins. Loss of TET1 causes loss of OGT from chromatin [25] and  
462 induces similar changes in transcription in both wild-type mESCs and mESCs lacking DNA  
463 methylation [42]. This raises the possibility that TET proteins may recruit OGT to chromatin to  
464 regulate gene expression independent of 5mC oxidation. Consistent with this possibility, OGT  
465 modifies many transcription factors and chromatin regulators in mESCs [43](Fig. 7). Thus it may  
466 be that the stable OGT-TET1 interaction promotes both regulation of TET1 activity by *O*-  
467 GlcNAcylation as well as recruitment of OGT to chromatin. Notably, our results show that TET1  
468 D2018A does not rescue 5hmC levels in *tet2/3<sup>DM</sup>* zebrafish embryos to the same extent as the  
469 wild type protein, suggesting that at least part of the role of the OGT-TET1 interaction *in vivo* is  
470 regulation of TET1 activity.

471 The D2018A mutation reduced, but did not completely disrupt, the OGT-TET1  
472 interaction in mESCs. In this cell type, TET1 is found in high molecular weight complexes that  
473 contain OGT, TET2, and the epigenetic regulator HCF1 [25]. In addition to TET1, OGT can  
474 directly interact with TET2 [26,27] and HCF1 [44] and TET2 co-IPs with TET1 [25]. Given the  
475 robust inhibition of the OGT-TET1 interaction by the D2018A mutation in multiple other  
476 contexts, our data are consistent with a scenario in which the D2018A mutation disrupts the  
477 direct interaction between OGT and TET1 in mESCs. However, some OGT remains associated in  
478 a co-IP assay through interactions with TET2 and/or HCF1. It is also possible that OGT interacts  
479 with the N-terminus of TET1, so that the D2018A mutation cripples but does not prevent the  
480 interaction with full-length TET1. This scenario is unlikely, however, since multiple studies have  
481 failed to identify any OGT binding capability outside the catalytic domains of TETs [27,34,45].

482

#### 483 **Regulation of TETs by OGT in development**

484 Our result that wild type TET1, but not TET1 carrying a mutation that can impair  
485 interaction with OGT, can rescue *tet2/3<sup>DM</sup>* zebrafish suggests that OGT regulation of TET  
486 enzymes may play a role in development. The importance of both TET proteins and OGT in  
487 development has been thoroughly established. Zebrafish lacking *tet2* and *tet3* die as larvae  
488 [30], and knockout of *Tet* genes in mice yields developmental phenotypes of varying severities,  
489 with knockout of all three *Tets* together being embryonic lethal [33,37,38,46]. Similarly, OGT is  
490 absolutely essential for development in mice [47], zebrafish [48], and *Drosophila* [49], though  
491 its vast number of targets have made it difficult to narrow down more specifically why OGT is  
492 necessary. Our results suggest that the function of the TET-OGT interaction in development  
493 may be two-fold. First, it may regulate TET enzyme activity. Second, OGT association with TETs  
494 may direct OGT to specific regions of the genome, facilitating O-GlcNAcylation of other  
495 transcriptional regulators in a site-specific manner (Fig. 7).

496

### 497 **A connection between metabolism and the epigenome**

498 OGT has been proposed to act as a metabolic sensor because its cofactor, UDP-GlcNAc,  
499 is synthesized via the hexosamine biosynthetic pathway (HBP), which is fed by pathways  
500 metabolizing glucose, amino acids, fatty acids, and nucleotides [23]. UDP-GlcNAc levels change  
501 in response to flux through these pathways [50-52], leading to the hypothesis that OGT activity  
502 may vary in response to the nutrient status of the cell. Thus the enhancement of TET1 activity  
503 by OGT and the significant overlap of the two enzymes on chromatin [25] suggest a model in  
504 which OGT may regulate the epigenome in response to nutrient status by controlling TET1  
505 activity (Fig. 7).

506

507

### 508 **Acknowledgments**

509 We thank Diego Pasini for the OGT++ mESCs, Miguel Ramalho-Santos for the FLAG-TET1  
510 CD plasmid, and Suzanne Walker for the His-OGT plasmid. We thank Leeanne Goodrich, Richard  
511 Yan, Christopher Agnew, and Sy Redding for technical assistance. We thank all members of the  
512 Panning lab for valuable ideas and discussion. This work was supported by R01 GM088506 (BP),  
513 NCI grant P30 CA008748 (MG), and funding from the Geoffrey Beene Cancer Research Center of  
514 Memorial Sloan-Kettering Cancer Center (MG). JH was supported by the California Institute for  
515 Regenerative Medicine Predoctoral Fellowship TG2-01153.

516

517

### 518 **Competing Financial Interests**

519 The authors declare no competing financial interests.

520

521

### 522 **References**

523

- 524 1. Guibert S, Weber M. Functions of DNA methylation and hydroxymethylation in  
525 mammalian development. *Curr Top Dev Biol*. Elsevier; 2013;104:47–83.
- 526 2. Smith ZD, Meissner A. DNA methylation: roles in mammalian development. *Nature*

- 527           Reviews Genetics. 2013 Mar;14(3):204–20.
- 528    3.    Tahiliani M, Koh KP, Shen Y, Pastor WA, Bandukwala H, Brudno Y, Agarwal S, Iyer LM, Liu  
529           DR, Aravind L, Rao A. Conversion of 5-Methylcytosine to 5-Hydroxymethylcytosine in  
530           Mammalian DNA by MLL Partner TET1. *Science*. 2009 May 14;324(5929):930–5.
- 531    4.    Ito S, D’Alessio AC, Taranova OV, Hong K, Sowers LC, Zhang Y. Role of Tet proteins in 5mC  
532           to 5hmC conversion, ES-cell self-renewal and inner cell mass specification. *Nature*. 2010  
533           Aug 26;466(7310):1129–33.
- 534    5.    Kriaucionis S, Heintz N. The nuclear DNA base 5-hydroxymethylcytosine is present in  
535           Purkinje neurons and the brain. *Science*. 2009 May 15;324(5929):929–30.
- 536    6.    He Y-F, Li B-Z, Li Z, Liu P, Wang Y, Tang Q, Ding J, Jia Y, Chen Z, Li L, Sun Y, Li X, Dai Q, Song  
537           C-X, Zhang K, He C, Xu G-L. Tet-mediated formation of 5-carboxylcytosine and its excision  
538           by TDG in mammalian DNA. *Science*. 2011 Sep 2;333(6047):1303–7.
- 539    7.    Ito S, Shen L, Dai Q, Wu SC, Collins LB, Swenberg JA, He C, Zhang Y. Tet proteins can  
540           convert 5-methylcytosine to 5-formylcytosine and 5-carboxylcytosine. *Science*. 2011 Sep  
541           2;333(6047):1300–3.
- 542    8.    Guo JU, Su Y, Zhong C, Ming G-L, Song H. Hydroxylation of 5-methylcytosine by TET1  
543           promotes active DNA demethylation in the adult brain. *Cell*. 2011 Apr 29;145(3):423–34.
- 544    9.    Cortellino S, Xu J, Sannai M, Moore R, Caretti E, Cigliano A, Le Coz M, Devarajan K,  
545           Wessels A, Soprano D, Abramowitz LK, Bartolomei MS, Rambow F, Bassi MR, Bruno T,  
546           Fanciulli M, Renner C, Klein-Szanto AJ, Matsumoto Y, Kobi D, Davidson I, Alberti C, Larue  
547           L, Bellacosa A. Thymine DNA glycosylase is essential for active DNA demethylation by  
548           linked deamination-base excision repair. *Cell*. 2011 Jul 8;146(1):67–79.
- 549    10.   Gao Y, Chen J, Li K, Wu T, Huang B, Liu W, Kou X, Zhang Y, Huang H, Jiang Y, Yao C, Liu X,  
550           Lu Z, Xu Z, Kang L, Chen J, Wang H, Cai T, Gao S. Replacement of Oct4 by Tet1 during iPSC  
551           induction reveals an important role of DNA methylation and hydroxymethylation in  
552           reprogramming. *Cell Stem Cell*. 2013 Apr 4;12(4):453–69.
- 553    11.   Weber AR, Krawczyk C, Robertson AB, Kuśnierczyk A, Vågbø CB, Schuermann D,  
554           Klungland A, Schär P. Biochemical reconstitution of TET1-TDG-BER-dependent active DNA  
555           demethylation reveals a highly coordinated mechanism. *Nature Communications*. 2016  
556           Mar 2;7:10806.
- 557    12.   Bachman M, Uribe-Lewis S, Yang X, Williams M, Murrell A, Balasubramanian S. 5-  
558           Hydroxymethylcytosine is a predominantly stable DNA modification. *Nature Chemistry*.  
559           2014 Dec;6(12):1049–55.
- 560    13.   Bachman M, Uribe-Lewis S, Yang X, Burgess HE, Iurlaro M, Reik W, Murrell A,  
561           Balasubramanian S. 5-Formylcytosine can be a stable DNA modification in mammals.

- 562 Nature Publishing Group. 2015 Aug;11(8):555–7.
- 563 14. Spruijt CG, Gnerlich F, Smits AH, Pfaffeneder T, Jansen PWTC, Bauer C, Münzel M,  
564 Wagner M, Müller M, Khan F, Eberl HC, Mensinga A, Brinkman AB, Lephikov K, Müller U,  
565 Walter J, Boelens R, van Ingen H, Leonhardt H, Carell T, Vermeulen M. Dynamic readers  
566 for 5-(hydroxy)methylcytosine and its oxidized derivatives. *Cell*. 2013 Feb  
567 28;152(5):1146–59.
- 568 15. Haltiwanger RS, Holt GD, Hart GW. Enzymatic addition of O-GlcNAc to nuclear and  
569 cytoplasmic proteins. Identification of a uridine diphospho-N-acetylglucosamine:peptide  
570 beta-N-acetylglucosaminyltransferase. *Journal of Biological Chemistry*. 1990 Feb  
571 15;265(5):2563–8.
- 572 16. Hanover JA, Krause MW, Love DC. Bittersweet memories: linking metabolism to  
573 epigenetics through O-GlcNAcylation. *Nat Rev Mol Cell Biol*. 2012 Apr 23;13(5):312–21.
- 574 17. Lewis BA, Hanover JA. O-GlcNAc and the epigenetic regulation of gene expression. *J Biol*  
575 *Chem*. 2014 Dec 12;289(50):34440–8.
- 576 18. Hardivillé S, Hart GW. Nutrient regulation of gene expression by O-GlcNAcylation of  
577 chromatin. *Current Opinion in Chemical Biology*. 2016 Aug;33:88–94.
- 578 19. Bullen JW, Balsbaugh JL, Chanda D, Shabanowitz J, Hunt DF, Neumann D, Hart GW. Cross-  
579 talk between two essential nutrient-sensitive enzymes: O-GlcNAc transferase (OGT) and  
580 AMP-activated protein kinase (AMPK). *J Biol Chem*. 2014 Apr 11;289(15):10592–606.
- 581 20. Ruan H-B, Singh JP, Li M-D, Wu J, Yang X. Cracking the O-GlcNAc code in metabolism.  
582 *Trends Endocrinol Metab*. 2013 Jun;24(6):301–9.
- 583 21. Durning SP, Flanagan-Steet H, Prasad N, Wells L. O-Linked  $\beta$ -N-acetylglucosamine (O-  
584 GlcNAc) Acts as a Glucose Sensor to Epigenetically Regulate the Insulin Gene in  
585 Pancreatic Beta Cells. *J Biol Chem*. 2016 Jan 29;291(5):2107–18.
- 586 22. Hanover JA, Forsythe ME, Hennessey PT, Brodigan TM, Love DC, Ashwell G, Krause M. A  
587 *Caenorhabditis elegans* model of insulin resistance: altered macronutrient storage and  
588 dauer formation in an OGT-1 knockout. *Proceedings of the National Academy of*  
589 *Sciences*. 2005 Aug 9;102(32):11266–71.
- 590 23. Hart GW, Slawson C, Ramirez-Correa G, Lagerlof O. Cross talk between O-GlcNAcylation  
591 and phosphorylation: roles in signaling, transcription, and chronic disease. *Annu Rev*  
592 *Biochem*. 2011;80:825–58.
- 593 24. Levine ZG, Walker S. The Biochemistry of O-GlcNAc Transferase: Which Functions Make It  
594 Essential in Mammalian Cells? *Annu Rev Biochem*. 2016 Jun 2;85:631–57.
- 595 25. Vella P, Scelfo A, Jammula S, Chiacchiera F, Williams K, Cuomo A, Roberto A, Christensen

- 596 J, Bonaldi T, Helin K, Pasini D. Tet proteins connect the O-linked N-acetylglucosamine  
597 transferase Ogt to chromatin in embryonic stem cells. *Molecular Cell*. 2013 Feb  
598 21;49(4):645–56.
- 599 26. Deplus R, Delatte B, Schwinn MK, Defrance M, Méndez J, Murphy N, Dawson MA,  
600 Volkmar M, Putmans P, Calonne E, Shih AH, Levine RL, Bernard O, Mercher T, Solary E,  
601 Urh M, Daniels DL, Fuks F. TET2 and TET3 regulate GlcNAcylation and H3K4 methylation  
602 through OGT and SET1/COMPASS. *The EMBO Journal*. 2013 Mar 6;32(5):645–55.
- 603 27. Chen Q, Chen Y, Bian C, Fujiki R, Yu X. TET2 promotes histone O-GlcNAcylation during  
604 gene transcription. *Nature*. 2013 Jan 24;493(7433):561–4.
- 605 28. Shi F-T, Kim H, Lu W, He Q, Liu D, Goodell MA, Wan M, Songyang Z. Ten-eleven  
606 translocation 1 (Tet1) is regulated by O-linked N-acetylglucosamine transferase (Ogt) for  
607 target gene repression in mouse embryonic stem cells. *J Biol Chem*. 2013 Jul  
608 19;288(29):20776–84.
- 609 29. Ran FA, Hsu PD, Wright J, Agarwala V, Scott DA, Zhang F. Genome engineering using the  
610 CRISPR-Cas9 system. *Nature Protocols*. 2013 Oct 24;8(11):2281–308.
- 611 30. Li C, Lan Y, Schwartz-Orbach L, Korol E, Tahiliani M, Evans T, Goll MG. Overlapping  
612 Requirements for Tet2 and Tet3 in Normal Development and Hematopoietic Stem Cell  
613 Emergence. *CellReports*. 2015 Aug 18;12(7):1133–43.
- 614 31. Kalev-Zylinska ML, Horsfield JA, Flores MVC, Postlethwait JH, Vitas MR, Baas AM, Crosier  
615 PS, Crosier KE. Runx1 is required for zebrafish blood and vessel development and  
616 expression of a human RUNX1-CBF2T1 transgene advances a model for studies of  
617 leukemogenesis. *Development*. 2002 Apr;129(8):2015–30.
- 618 32. Thisse C, Thisse B. High-resolution in situ hybridization to whole-mount zebrafish  
619 embryos. *Nature Protocols*. 2008;3(1):59–69.
- 620 33. Dawlaty MM, Breiling A, Le T, Raddatz G, Barrasa MI, Cheng AW, Gao Q, Powell BE, Li Z,  
621 Xu M, Faull KF, Lyko F, Jaenisch R. Combined deficiency of Tet1 and Tet2 causes  
622 epigenetic abnormalities but is compatible with postnatal development. *Developmental*  
623 *Cell*. 2013 Feb 11;24(3):310–23.
- 624 34. Ito R, Katsura S, Shimada H, Tsuchiya H, Hada M, Okumura T, Sugawara A, Yokoyama A.  
625 TET3-OGT interaction increases the stability and the presence of OGT in chromatin.  
626 *Genes Cells*. 2014 Jan;19(1):52–65.
- 627 35. Hu L, Li Z, Cheng J, Rao Q, Gong W, Liu M, Shi YG, Zhu J, Wang P, Xu Y. Crystal structure of  
628 TET2-DNA complex: insight into TET-mediated 5mC oxidation. *Cell*. 2013 Dec  
629 19;155(7):1545–55.
- 630 36. Koh KP, Yabuuchi A, Rao S, Huang Y, Cunniff K, Nardone J, Laiho A, Tahiliani M, Sommer

- 631 CA, Mostoslavsky G, Lahesmaa R, Orkin SH, Rodig SJ, Daley GQ, Rao A. Tet1 and Tet2  
632 regulate 5-hydroxymethylcytosine production and cell lineage specification in mouse  
633 embryonic stem cells. *Cell Stem Cell*. 2011 Feb 4;8(2):200–13.
- 634 37. Dawlaty MM, Ganz K, Powell BE, Hu Y-C, Markoulaki S, Cheng AW, Gao Q, Kim J, Choi S-  
635 W, Page DC, Jaenisch R. Tet1 is dispensable for maintaining pluripotency and its loss is  
636 compatible with embryonic and postnatal development. *Cell Stem Cell*. 2011 Aug  
637 5;9(2):166–75.
- 638 38. Li Z, Cai X, Cai C-L, Wang J, Zhang W, Petersen BE, Yang F-C, Xu M. Deletion of Tet2 in  
639 mice leads to dysregulated hematopoietic stem cells and subsequent development of  
640 myeloid malignancies. *Blood*. 2011 Oct 27;118(17):4509–18.
- 641 39. Zhao Z, Chen L, Dawlaty MM, Pan F, Weeks O, Zhou Y, Cao Z, Shi H, Wang J, Lin L, Chen S,  
642 Yuan W, Qin Z, Ni H, Nimer SD, Yang F-C, Jaenisch R, Jin P, Xu M. Combined Loss of Tet1  
643 and Tet2 Promotes B Cell, but Not Myeloid Malignancies, in Mice. *CellReports*. 2015 Nov  
644 24;13(8):1692–704.
- 645 40. Huang Y, Chavez L, Chang X, Wang X, Pastor WA, Kang J, Zepeda-Martinez JA, Pape UJ,  
646 Jacobsen SE, Peters B, Rao A. Distinct roles of the methylcytosine oxidases Tet1 and Tet2  
647 in mouse embryonic stem cells. *Proceedings of the National Academy of Sciences*. 2014  
648 Jan 28;111(4):1361–6.
- 649 41. Fidalgo M, Huang X, Guallar D, Sanchez-Priego C, Valdes VJ, Saunders A, Ding J, Wu W-S,  
650 Clavel C, Wang J. Zfp281 Coordinates Opposing Functions of Tet1 and Tet2 in Pluripotent  
651 States. *Cell Stem Cell*. 2016 Sep 1;19(3):355–69.
- 652 42. Williams K, Christensen J, Pedersen MT, Johansen JV, Cloos PAC, Rappsilber J, Helin K.  
653 TET1 and hydroxymethylcytosine in transcription and DNA methylation fidelity. *Nature*.  
654 2011 May 19;473(7347):343–8.
- 655 43. Myers SA, Panning B, Burlingame AL. Polycomb repressive complex 2 is necessary for the  
656 normal site-specific O-GlcNAc distribution in mouse embryonic stem cells. *Proceedings of  
657 the National Academy of Sciences*. 2011 Jun 7;108(23):9490–5.
- 658 44. Capotosti F, Guernier S, Lammers F, Waridel P, Cai Y, Jin J, Conaway JW, Conaway RC,  
659 Herr W. O-GlcNAc transferase catalyzes site-specific proteolysis of HCF-1. *Cell*. 2011 Feb  
660 4;144(3):376–88.
- 661 45. Zhang Q, Liu X, Gao W, Li P, Hou J, Li J, Wong J. Differential Regulation of the Ten-Eleven  
662 Translocation (TET) Family of Dioxygenases by O-Linked  $\beta$ - N-Acetylglucosamine  
663 Transferase (OGT). *Journal of Biological Chemistry*. 2014 Feb 27;289(9):5986–96.
- 664 46. Dawlaty M. Loss of Tet Enzymes Compromises Proper Differentiation of Embryonic Stem  
665 Cells. 2014 Mar 13;:1–8.



- 666 47. Shafi R, Iyer SPN, Ellies LG, O'Donnell N, Marek K, Chiu D, Hart GW, Marth JD. The O-  
667 GlcNAc transferase gene resides on the X chromosome and is essential for  
668 embryonic stem cell viability and mouse ontogeny. *Proceedings of the National Academy  
669 of Sciences*. 2000 May 23;97(11):5735–9.
- 670 48. Webster DM, Webster DM, Teo C, Teo C, Sun Y, Sun Y, Wloga D, Wloga D, Gay S, Gay S,  
671 Klonowski KD, Klonowski KD, Wells L, Dougan ST, Dougan ST. O-GlcNAc modifications  
672 regulate cell survival and epiboly during zebrafish development. *BMC Dev Biol*.  
673 2009;9(1):28.
- 674 49. Ingham PW. A Gene That Regulates the Bithorax Complex Differentially in Larval and  
675 Cells of *Drosophila*. *Cell*. 1984 Jul 12;37:815–23.
- 676 50. Marshall S, Nadeau O, Yamasaki K. Dynamic Actions of Glucose and Glucosamine on  
677 Hexosamine Biosynthesis in Isolated Adipocytes: DIFFERENTIAL EFFECTS ON  
678 GLUCOSAMINE 6-PHOSPHATE, UDP-N-ACETYLGLUCOSAMINE, AND ATP LEVELS. *Journal  
679 of Biological Chemistry*. 2004 Aug 13;279(34):35313–9.
- 680 51. McClain DA. Hexosamines as mediators of nutrient sensing and regulation in diabetes.  
681 *Journal of Diabetes and its Complications*. 2002 Feb 20;16:72–80.
- 682 52. Weigert C, Klopfer K, Kausch C, Brodbeck K, Stumvoll M, Haring H, Schleicher E.  
683 Palmitate-Induced Activation of the Hexosamine Pathway in Human Myotubes Increased  
684 Expression of Glutamine:Fructose-6-Phosphate Aminotransferase. *Diabetes*. 2003 Mar  
685 6;52:1–7.

686

687

688

689

690

691

692

693

694

695

696

697

698

699

700

701

702

703

# Figure 1

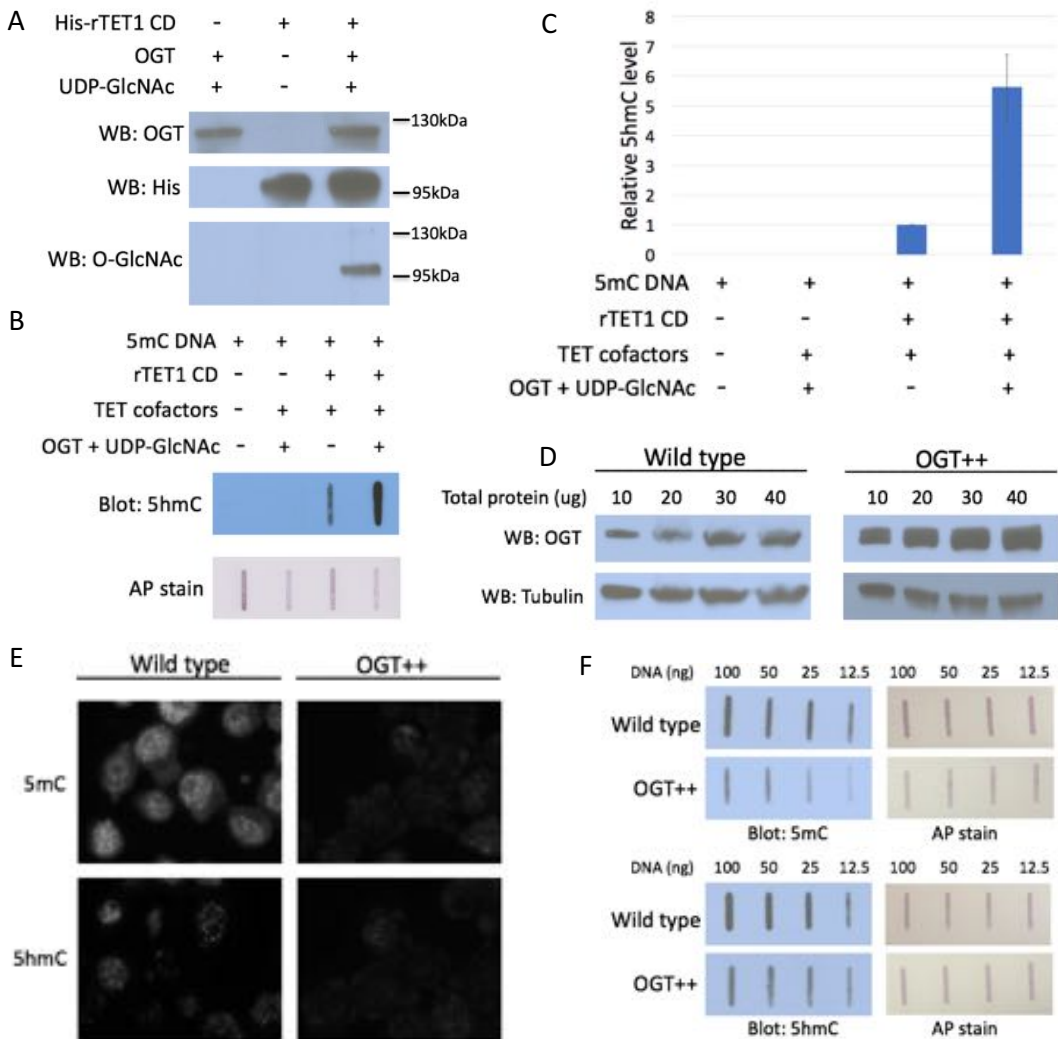


**Fig. 1: OGT enhances TET activity *in vitro* and in cells**

A) Western blot for OGT, rTET1 CD, and O-GlcNAc in *in vitro* O-GlcNAcylation reaction demonstrating UDP-GlcNAc dependent TET1 CD O-GlcNAcylation. B) 5hmC slot blot of biotinylated 5mC containing lambda DNA from rTET1 CD activity assays. Alkaline phosphatase staining was used to detect biotin as a loading control. C) Quantification of 5hmC levels from four slot blots. All results normalized to TET1 CD without UDP-GlcNAc and OGT. D) Western blot of 10-40ug lysate from wild type and OGT overexpressing (OGT++) mESCs, showing increased OGT levels in OGT++ mESCs. E) Immunofluorescence comparing 5mC (upper) and 5hmC (lower) levels in wild type vs. OGT++ mESCs. F) Slot blots for 5mC and 5hmC of 12.5-100 ng genomic DNA from wild type and OGT++ mESCs. Equal amounts of biotinylated plasmid DNA were added to each gDNA dilution and alkaline phosphatase staining was used to detect biotin as a loading control.

704 **Fig. 1: OGT enhances TET activity *in vitro* and in cells**

705 A) Western blot for OGT, rTET1 CD, and *O*-GlcNAc in *in vitro* *O*-GlcNAcylation reaction  
706 demonstrating UDP-GlcNAc dependent TET1 CD *O*-GlcNAcylation. B) 5hmC slot blot of  
707 biotinylated 5mC containing lambda DNA from rTET1 CD activity assays. Alkaline phosphatase  
708 staining was used to detect biotin as a loading control. C) Quantification of 5hmC levels from  
709 four slot blots. All results normalized to TET1 CD without UDP-GlcNAc and OGT. D) Western blot  
710 of 10-40ug lysate from wild type and OGT overexpressing (OGT++) mESCs, showing increased  
711 OGT levels in OGT++ mESCs. E) Immunofluorescence comparing 5mC (upper) and 5hmC (lower)  
712 levels in wild type vs. OGT++ mESCs. F) Slot blots for 5mC and 5hmC of 12.5-100 ng genomic  
713 DNA from wild type and OGT++ mESCs. Equal amounts of biotinylated plasmid DNA were added  
714 to each gDNA dilution and alkaline phosphatase staining was used to detect biotin as a loading  
715 control.

716  
717  
718  
719  
720  
721  
722  
723  
724  
725  
726  
727  
728  
729  
730  
731  
732  
733  
734  
735  
736  
737  
738  
739  
740  
741  
742  
743  
744  
745  
746  
747

# Figure 2

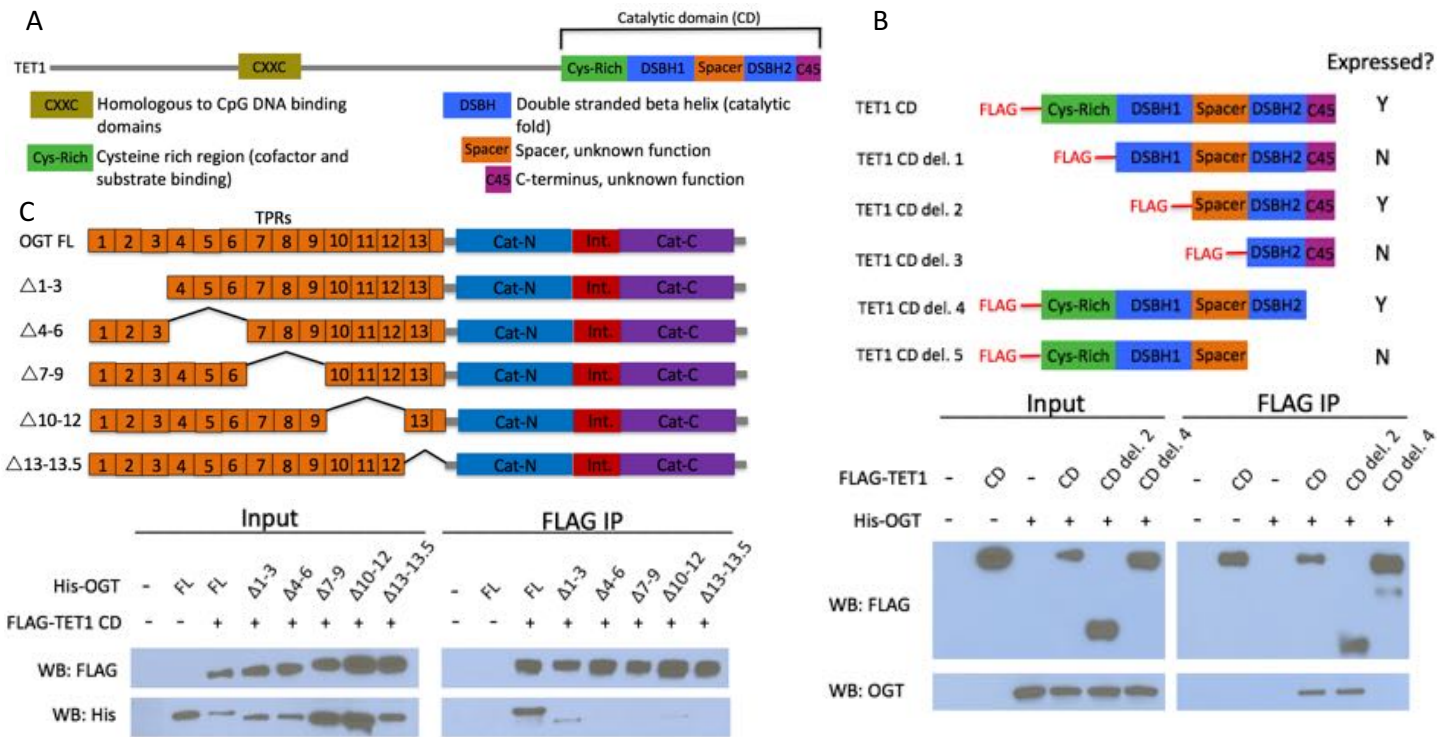


**Fig. 2: The short TET1 C-terminus is required for interaction with OGT**

A) Domain architecture of TET1. B) Diagram of FLAG-tagged TET1 CD constructs expressed in HEK293T cells (upper). FLAG and OGT western blot of inputs and FLAG IPs from HEK293T cells transiently expressing FLAG-TET1 CD truncations and His-OGT (lower). C) Diagram of His-tagged OGT constructs expressed in HEK293T cells (upper). FLAG and His western blot of input and FLAG IPs from HEK293T cells transiently expressing FLAG-TET1 CD and His-OGT TPR deletions (lower).

748 **Fig. 2: The short TET1 C-terminus is required for interaction with OGT**

749 A) Domain architecture of TET1. B) Diagram of FLAG-tagged TET1 CD constructs expressed in  
750 HEK293T cells (upper). FLAG and OGT western blot of inputs and FLAG IPs from HEK293T cells  
751 transiently expressing FLAG-TET1 CD truncations and His-OGT (lower). C) Diagram of His-tagged  
752 OGT constructs expressed in HEK293T cells (upper). FLAG and His western blot of input and  
753 FLAG IPs from HEK293T cells transiently expressing FLAG-TET1 CD and His-OGT TPR deletions  
754 (lower).

755  
756  
757  
758  
759  
760  
761  
762  
763  
764  
765  
766  
767  
768  
769  
770  
771  
772  
773  
774  
775  
776  
777  
778  
779  
780  
781  
782  
783  
784  
785  
786  
787  
788  
789  
790  
791

# Figure 3

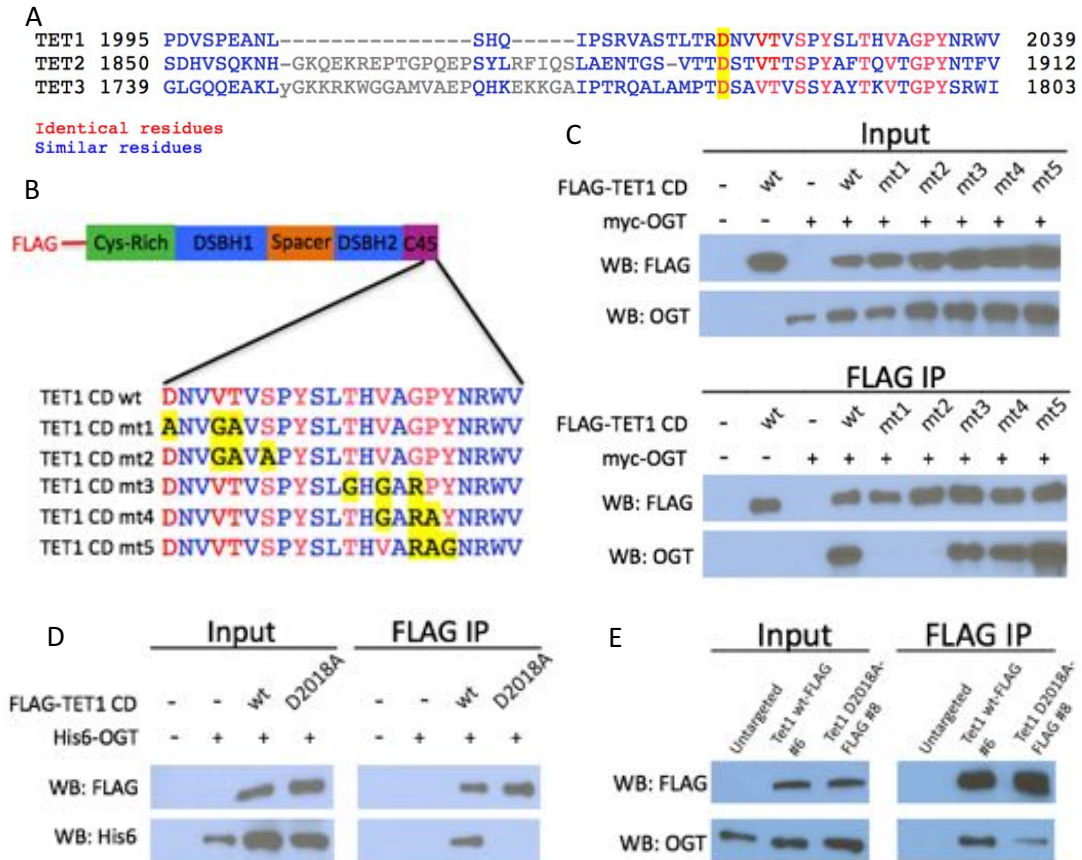


**Fig. 3: Conserved residues in the TET1 C45 are necessary for the TET1-OGT interaction**

A) Alignment of the C-termini of mouse TETs 1, 2, and 3. A conserved aspartate residue mutated in D and E is highlighted. B) Diagram of FLAG-tagged TET1 CD constructs expressed in HEK293T cells. C) FLAG and OGT western blot of inputs and FLAG IPs from HEK293T cells transiently expressing FLAG-TET1 CD triple point mutants and His-OGT. D) FLAG and OGT western blot of inputs and FLAG IPs from HEK293T cells transiently expressing His-OGT and FLAG-TET1 CD or FLAG-TET1 CD D2018A. E) FLAG and OGT western blot of inputs and FLAG IPs from mESCs in which a FLAG tag or a FLAG tag and the D2018A mutation were introduced into both copies of *Tet1* (Fig. S4).

792 **Fig. 3: Conserved residues in the TET1 C45 are necessary for the TET1-OGT interaction**  
793 A) Alignment of the C-termini of mouse TETs 1, 2, and 3. A conserved aspartate residue  
794 mutated in D and E is highlighted. B) Diagram of FLAG-tagged TET1 CD constructs expressed in  
795 HEK293T cells. C) FLAG and OGT western blot of inputs and FLAG IPs from HEK293T cells  
796 transiently expressing FLAG-TET1 CD triple point mutants and His-OGT. D) FLAG and OGT  
797 western blot of inputs and FLAG IPs from HEK293T cells transiently expressing His-OGT and  
798 FLAG-TET1 CD or FLAG-TET1 CD D2018A. E) FLAG and OGT western blot of inputs and FLAG IPs  
799 from mESCs in which a FLAG tag or a FLAG tag and the D2018A mutation were introduced into  
800 both copies of *Tet1* (Fig. S4).

801  
802  
803  
804  
805  
806  
807  
808  
809  
810  
811  
812  
813  
814  
815  
816  
817  
818  
819  
820  
821  
822  
823  
824  
825  
826  
827  
828  
829  
830  
831  
832  
833  
834  
835

# Figure 4

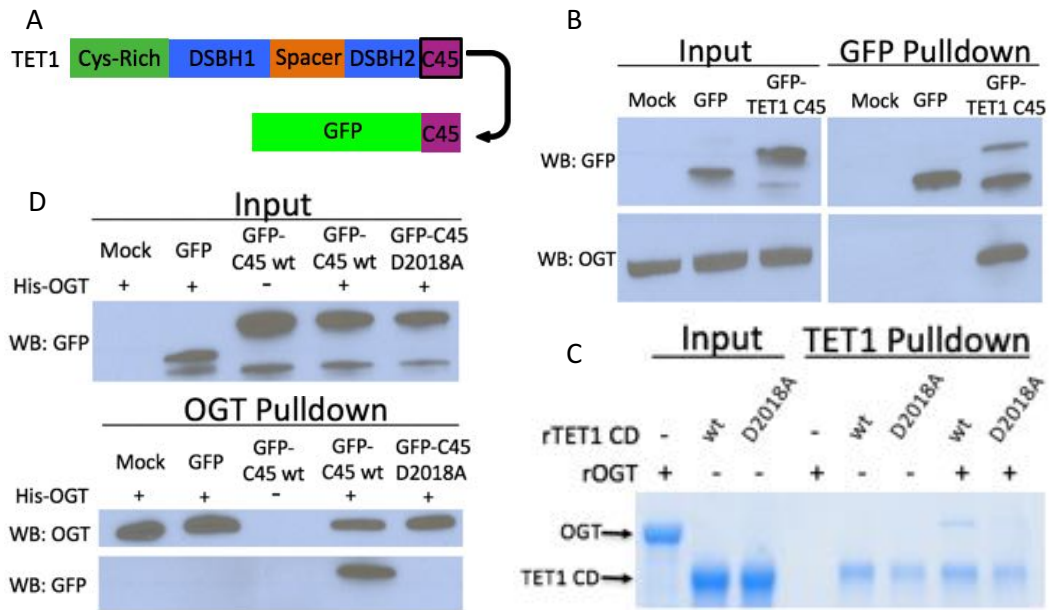


**Fig. 4: The TET1 C45 is sufficient for interaction with OGT in cells and *in vitro***

A) Schematic of the TET1 C45 fusion to the C-terminus of GFP. B) GFP and OGT western blot of inputs and GFP IPs from HEK293T cells transiently expressing GFP or GFP-TET1 C45. C) Coomassie stained protein gel of inputs and TET1 IPs from *in vitro* binding reactions containing rOGT and rTET1 CD wild type or D2018A. D) GFP and OGT western blot of inputs and OGT IPs from *in vitro* binding reactions containing rOGT and *in vitro* translated GFP constructs.



836 **Fig. 4: The TET1 C45 is sufficient for interaction with OGT in cells and *in vitro***  
837 A) Schematic of the TET1 C45 fusion to the C-terminus of GFP. B) GFP and OGT western blot of  
838 inputs and GFP IPs from HEK293T cells transiently expressing GFP or GFP-TET1 C45. C)  
839 Coomassie stained protein gel of inputs and TET1 IPs from *in vitro* binding reactions containing  
840 rOGT and rTET1 CD wild type or D2018A. D) GFP and OGT western blot of inputs and OGT IPs  
841 from *in vitro* binding reactions containing rOGT and *in vitro* translated GFP constructs.

842  
843  
844  
845  
846  
847  
848  
849  
850  
851  
852  
853  
854  
855  
856  
857  
858  
859  
860  
861  
862  
863  
864  
865  
866  
867  
868  
869  
870  
871  
872  
873  
874  
875  
876  
877  
878  
879

# Figure 5

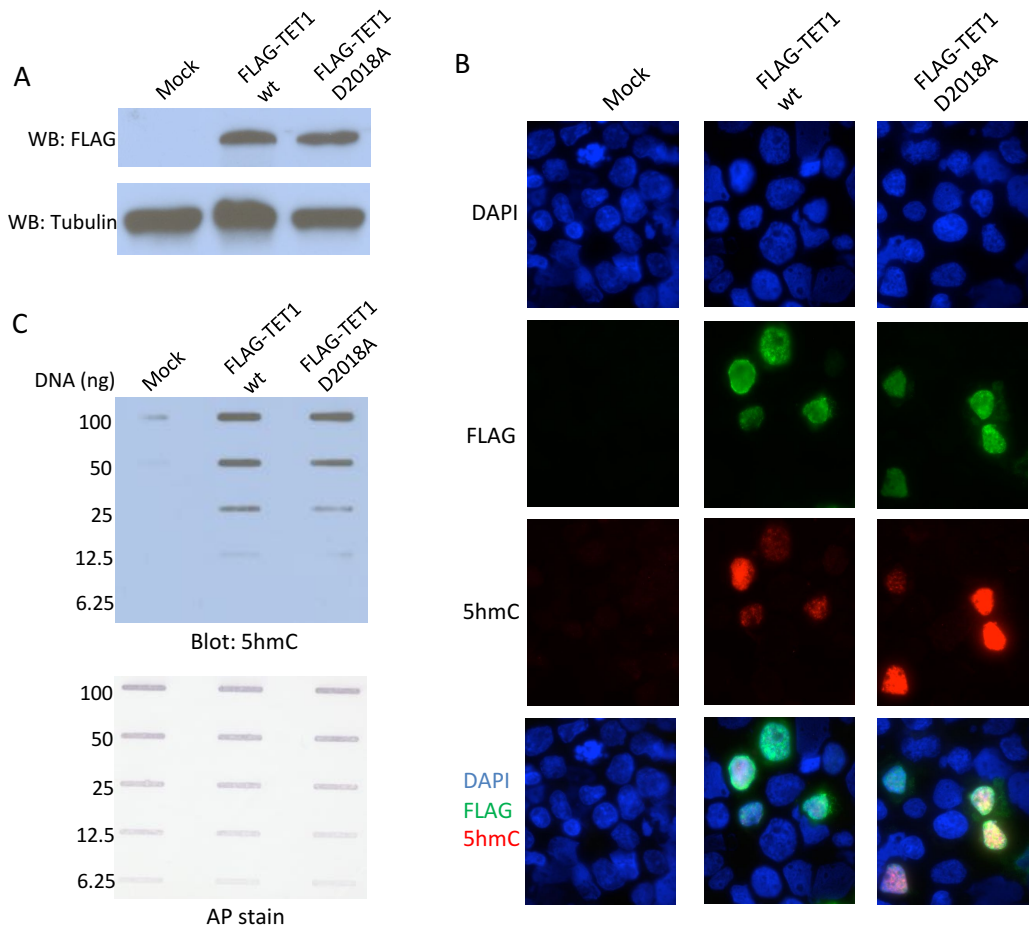


## Fig. 5: TET1 D2018A is active in HEK293T cells

A) FLAG western blot of HEK293T cell lysates transiently expressing FLAG-TET1 wild type or D2018A. Western blot for Tubulin was performed as a loading control. B) Immunofluorescence for FLAG (green) and 5hmC (red) in HEK293T cells transiently expressing FLAG-TET1 wild type or D2018A. DAPI (blue) was used to stain nuclei. C) 5hmC slot blot of 6.25-100ng genomic DNA from HEK293T cells transiently expressing FLAG-TET1 wild type or D2018A. Equal amounts of biotinylated plasmid DNA were added to each gDNA stock and diluted across the dilution series. Alkaline phosphatase staining was used to detect biotin as a loading and dilution control.

880 **Fig. 5: TET1 D2018A is active in HEK293T cells**

881 A) FLAG western blot of HEK293T cell lysates transiently expressing FLAG-TET1 wild type or  
882 D2018A. Western blot for Tubulin was performed as a loading control. B) Immunofluorescence  
883 for FLAG (green) and 5hmC (red) in HEK293T cells transiently expressing FLAG-TET1 wild type or  
884 D2018A. DAPI (blue) was used to stain nuclei. C) 5hmC slot blot of 6.25-100ng genomic DNA  
885 from HEK293T cells transiently expressing FLAG-TET1 wild type or D2018A. Equal amounts of  
886 biotinylated plasmid DNA were added to each gDNA stock and diluted across the dilution series.  
887 Alkaline phosphatase staining was used to detect biotin as a loading and dilution control.

888  
889  
890  
891  
892  
893  
894  
895  
896  
897  
898  
899  
900  
901  
902  
903  
904  
905  
906  
907  
908  
909  
910  
911  
912  
913  
914  
915  
916  
917  
918  
919  
920  
921  
922  
923

# Figure 6

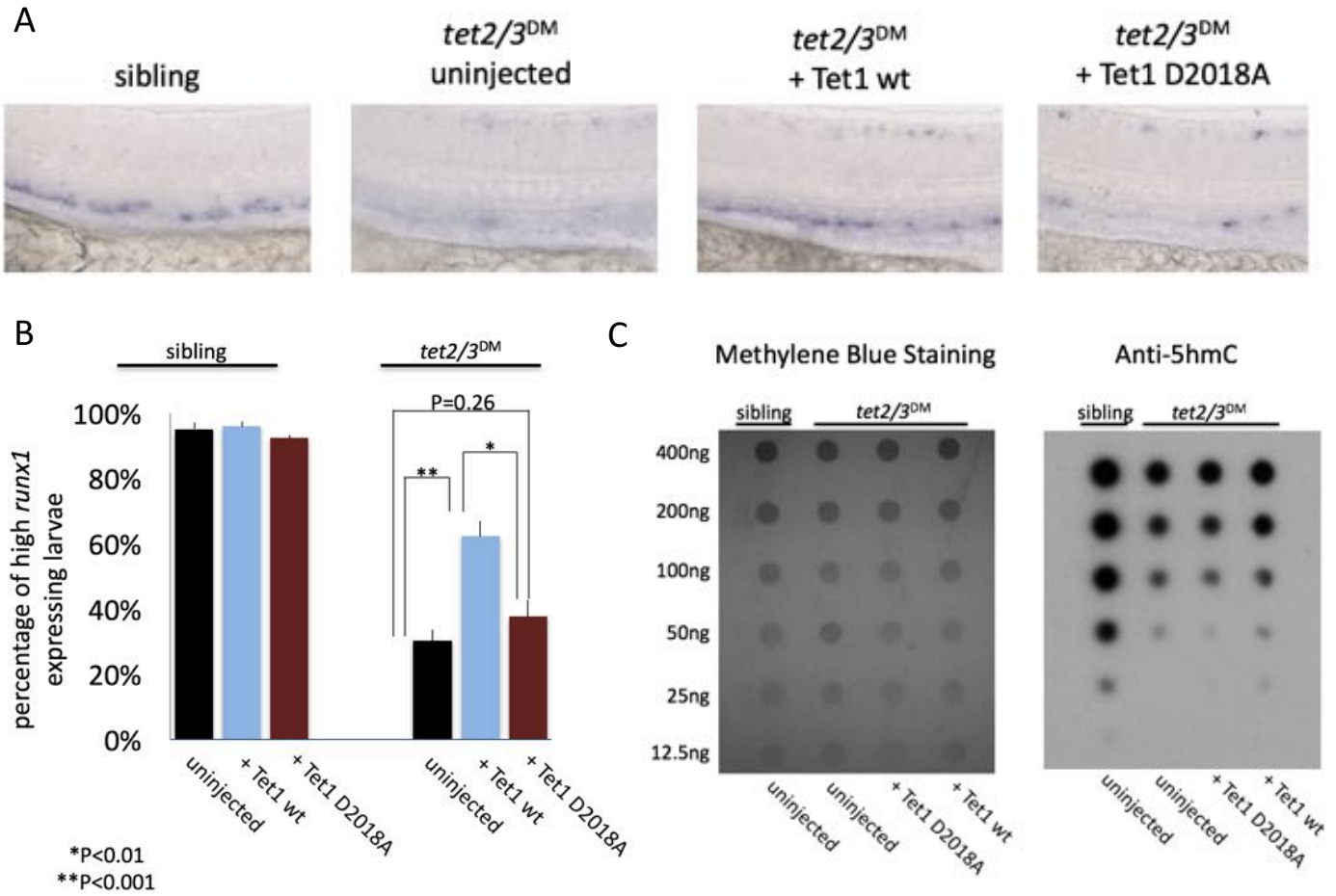


**Fig. 6: The interaction with OGT is required for TET1 activity in the zebrafish embryo**

A) Representative images of *runx1* labeling in the dorsal aorta of wild type or *tet2/3<sup>DM</sup>* zebrafish embryos, uninjected or injected with mRNA encoding Tet1 wild type or D2018A, B) Percentage of embryos with high *runx1* expression along the dorsal aorta. C) 5hmC dot blot of genomic DNA from wild type or *tet2/3<sup>DM</sup>* zebrafish embryos injected with Tet1 wild type or D2018A mRNA. Methylene blue was used as a loading control.

924 **Fig. 6: The interaction with OGT is required for TET1 activity in the zebrafish embryo**

925 A) Representative images of *runx1* labeling in the dorsal aorta of wild type or *tet2/3<sup>DM</sup>* zebrafish  
926 embryos, uninjected or injected with mRNA encoding Tet1 wild type or D2018A, B) Percentage  
927 of embryos with high *runx1* expression along the dorsal aorta. C) 5hmC dot blot of genomic  
928 DNA from wild type or *tet2/3<sup>DM</sup>* zebrafish embryos injected with Tet1 wild type or D2018A  
929 mRNA. Methylene blue was used as a loading control.

930  
931  
932  
933  
934  
935  
936  
937  
938  
939  
940  
941  
942  
943  
944  
945  
946  
947  
948  
949  
950  
951  
952  
953  
954  
955  
956  
957  
958  
959  
960  
961  
962  
963  
964  
965  
966  
967

# Figure 7

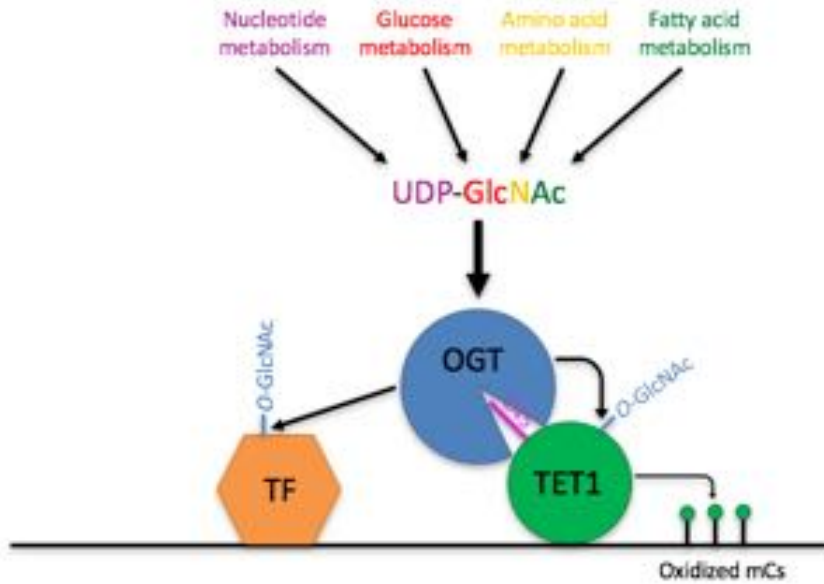


**Fig. 7:**

Model showing two roles of the TET1-OGT interaction in regulation of gene expression. OGT's activity is regulated by the abundance of its cofactor UDP-GlcNAc, whose synthesis depends on the abundance of various cellular metabolites. OGT (blue circle) binds to TET1 (large green circle) via the TET1 C45 (purple line). OGT modifies TET1 and regulates its catalytic activity (small green circles representing modified cytosines). At the same time, TET1 binding to DNA brings OGT into proximity of other DNA-bound transcription factors (orange hexagon), which OGT also modifies and regulates.

968 **Fig. 7:**

969 Model showing two roles of the TET1-OGT interaction in regulation of gene expression. OGT's  
970 activity is regulated by the abundance of its cofactor UDP-GlcNAc, whose synthesis depends on  
971 the abundance of various cellular metabolites. OGT (blue circle) binds to TET1 (large green  
972 circle) via the TET1 C45 (purple line). OGT modifies TET1 and regulates its catalytic activity  
973 (small green circles representing modified cytosines). At the same time, TET1 binding to DNA  
974 brings OGT into proximity of other DNA-bound transcription factors (orange hexagon), which  
975 OGT also modifies and regulates.

976

977

978

979

980

981

982

983

984

985

986

987

988

989

990

991

992

993

994

995

996

997

998

999

1000

1001

1002

1003

1004

1005

1006

1007

1008

1009

1010

1011

# Figure S1

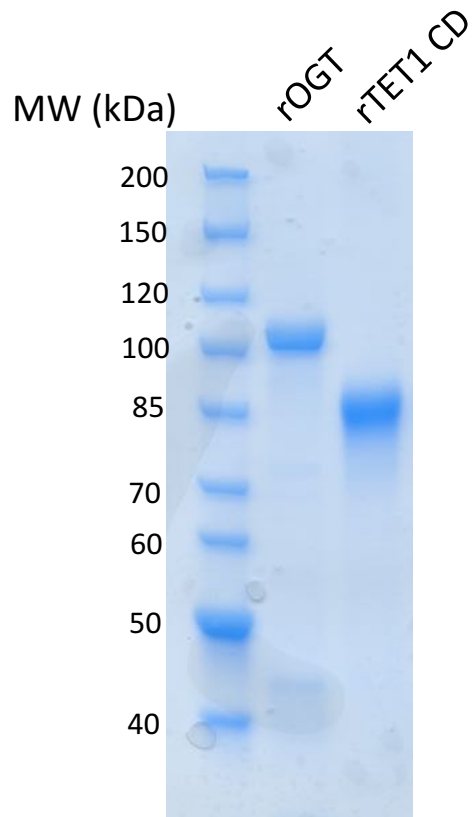



**Fig. S1:**

Coomassie stained SDS-PAGE gel of purified rOGT and rTET1 CD.



1012 **Fig. S1:**  
1013 Coomassie stained SDS-PAGE gel of purified rOGT and rTET1 CD.  
1014  
1015  
1016  
1017  
1018  
1019  
1020  
1021  
1022  
1023  
1024  
1025  
1026  
1027  
1028  
1029  
1030  
1031  
1032  
1033  
1034  
1035  
1036  
1037  
1038  
1039  
1040  
1041  
1042  
1043  
1044  
1045  
1046  
1047  
1048  
1049  
1050  
1051  
1052  
1053  
1054  
1055

# Figure S2

5mC DNA	+	+	+
rTET1 CD	-	+	+
TET cofactors	-	-	+
Blot: 5hmC			

**Fig. S2:**

5hmC slot blot of biotinylated 5mC containing lambda DNA from rTET1 CD activity assays.

1056 **Fig. S2:**  
1057 5hmC slot blot of biotinylated 5mC containing lambda DNA from rTET1 CD activity assays.

1058  
1059  
1060  
1061  
1062  
1063  
1064  
1065  
1066  
1067  
1068  
1069  
1070  
1071  
1072  
1073  
1074  
1075  
1076  
1077  
1078  
1079  
1080  
1081  
1082  
1083  
1084  
1085  
1086  
1087  
1088  
1089  
1090  
1091  
1092  
1093  
1094  
1095  
1096  
1097  
1098  
1099

# Figure S3

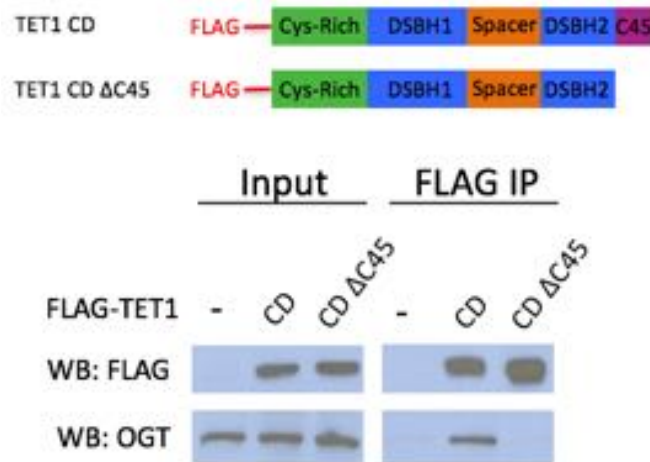


**Fig. S3:**

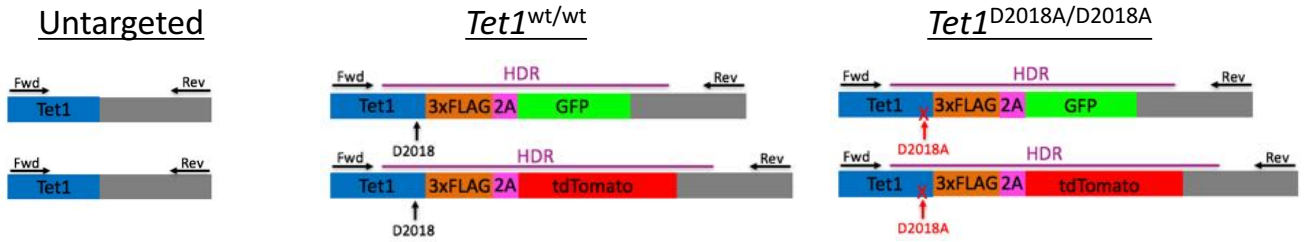
FLAG and OGT western blot of inputs and FLAG IPs from HEK293T cells transiently expressing FLAG-TET1 CD or FLAG-TET1 CD  $\Delta$ C45 (diagrammed in the upper panel).

1100 **Fig. S3:**  
1101 FLAG and OGT western blot of inputs and FLAG IPs from HEK293T cells transiently expressing  
1102 FLAG-TET1 CD or FLAG-TET1 CD  $\Delta$ C45 (diagrammed in the upper panel).

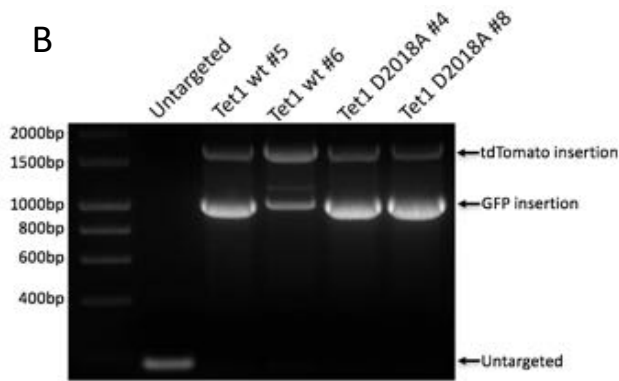
1103  
1104  
1105  
1106  
1107  
1108  
1109  
1110  
1111  
1112  
1113  
1114  
1115  
1116  
1117  
1118  
1119  
1120  
1121  
1122  
1123  
1124  
1125  
1126  
1127  
1128  
1129  
1130  
1131  
1132  
1133  
1134  
1135  
1136  
1137  
1138  
1139  
1140  
1141  
1142  
1143

# Figure S4

A



B



C

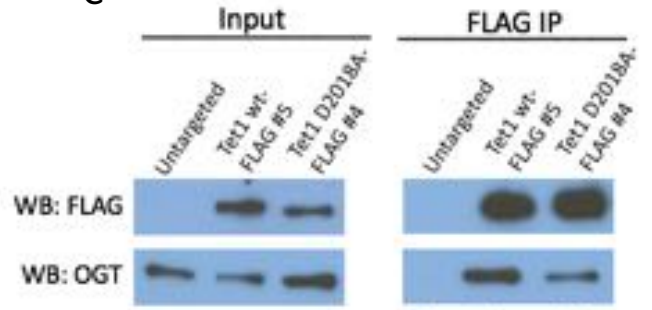


**Fig. S4:**

A) Schematic of mESC lines. DNA encoding a 3xFLAG tag was added to the 3' end of both alleles of *Tet1*, followed by a 2A sequence and a fluorescent protein (GFP or tdTomato). The 2A sequence causes ribosome skipping, resulting in separate translation of TET1-3xFLAG and 2A-GFP or 2A-tdTomato. Purple line: template used for homology-directed repair (HDR). Horizontal arrows: primers used for PCR genotyping. Vertical arrows: D2018 residue. B) PCR genotyping of independently derived, clonal, targeted mESC lines using primers indicated in A. C) FLAG and OGT western blot of inputs and FLAG IPs from a second set of mESC lines in which a FLAG tag or a FLAG tag and the D2018A mutation were introduced into both copies of *Tet1*.

1144 **Fig. S4:**

1145 A) Schematic of mESC lines. DNA encoding a 3xFLAG tag was added to the 3' end of both alleles  
1146 of *Tet1*, followed by a 2A sequence and a fluorescent protein (GFP or tdTomato). The 2A  
1147 sequence causes ribosome skipping, resulting in separate translation of TET1-3xFLAG and 2A-  
1148 GFP or 2A-tdTomato. Purple line: template used for homology-directed repair (HDR).  
1149 Horizontal arrows: primers used for PCR genotyping. Vertical arrows: D2018 residue. B) PCR  
1150 genotyping of independently derived, clonal, targeted mESC lines using primers indicated in A.  
1151 C) FLAG and OGT western blot of inputs and FLAG IPs from a second set of mESC lines in which  
1152 a FLAG tag or a FLAG tag and the D2018A mutation were introduced into both copies of *Tet1*.

1153  
1154  
1155  
1156  
1157  
1158  
1159  
1160  
1161  
1162  
1163  
1164  
1165  
1166  
1167  
1168  
1169  
1170  
1171  
1172  
1173  
1174  
1175  
1176  
1177  
1178  
1179  
1180  
1181  
1182  
1183  
1184  
1185  
1186  
1187

1188 **Table S1:**  
1189 **Primers used for creating and genotyping mESC lines**  
1190

<b>Name</b>	<b>Purpose</b>	<b>Sequence</b>
WtAmpFwd	Forward primer for amplifying Tet1 wt Gene Blocks to make HDR template	atcaaccttaacccgagaca
MutAmpFwd	Forward primer for amplifying Tet1 D2018A Gene Blocks to make HDR template	tcaaccttaacccgagcc
AmpRev	Reverse primer for amplifying Tet1 wt and D2018A Gene Blocks to make HDR template	cttttaacagcaccgaaa
GenotypeFwd	Forward primer for genotyping Tet1 allele	tgatgtatccccgaagc
GenotypeRev	Reverse primer for genotyping Tet1 allele	cccactacaccacattagca

1191  
1192  
1193  
1194  
1195  
1196  
1197  
1198  
1199  
1200  
1201  
1202  
1203  
1204  
1205  
1206  
1207  
1208  
1209  
1210  
1211  
1212  
1213  
1214  
1215  
1216  
1217  
1218  
1219  
1220  
1221



1222 **Table S2:**  
 1223 **Gene blocks amplified to make HDR templates**

Name	Sequence
Tet1 wt-3xF-T2A-GFP	gcagaccgggagtgctctgatgtatccccgaagccaatttatcacaccaaattccttctcgagttgcatcaacctt aaccgagacaatgttgttaccgtgtcccatactctctcactcatgttgcgggaccataacaatcgttgggtcgact acaaagaccatgacgggtgattataaagatcatgatatcgattacaaggatgacgatgacaaggggaagcgggagag ggagaggaagtctgctaacaatgacgggtgacgtcgaggagaatcctggacctgtgagcaagggcgaggagctgtt caccggggtggtgcccatcctggtcgagctggacggcgacgtaaaccggccacaagttcagcgtgtccggcgagg gcgagggcgatgccacctacggcaagctgacctgaaatattttgacgacaggggaagctgccctgacctggc ccacctcgttacgacctaacatatggcgtgagtgcttcagccgctaccggatcatatgaagcaacacgactt cttaagtacgcatgcccgaaggctacgtccaggagcgaccatcttctcaaggacgacggcaactacaagac ccgcccggaggtgaagttcgagggcgacacctggtgaaccgcatcgagctgaagggcatcgacttcaaggagg acggcaacatcctggggcacaagctggagtacaactacaacagccacaacgtctatatcatggccgacaagcag aagaacggcatcaaggtgaacttcaagatccgccacaacatcgaggacggcagcgtgagctcggcaccacta ccagcagaacacccccatcggcgacggccccgtgctgctgcccgacaaccactacctgagcaccagtcggcct gagcaaagaccccaacgagaagcgcgatcacatggtcctgctggagtctgtgaccgcccgggatcactctcg catggacgagctgtacaagtaaaagcttctctcatgtaatgcatgctgctgctgctgcccgacaaccactac ctgagcaccagtcggccttggtttgtttttgttttttccgggtgctgttaaaaagaaagtcattctgtgttactgtagctt gtttgc ccatttc
Tet1 D2018A-3xF-T2A-GFP	gcagaccgggagtgctctgatgtatccccgaagccaatttatcacaccaaattccttctcgagttgcatcaacctt aaccgagccaatgttgttaccgtgtcccatactctctcactcatgttgcgggaccataacaatcgttgggtcgact acaaagaccatgacgggtgattataaagatcatgatatcgattacaaggatgacgatgacaaggggaagcgggagag ggagaggaagtctgctaacaatgacgggtgacgtcgaggagaatcctggacctgtgagcaagggcgaggagctgtt caccggggtggtgcccatcctggtcgagctggacggcgacgtaaaccggccacaagttcagcgtgtccggcgagg gcgagggcgatgccacctacggcaagctgacctgaaatattttgacgacaggggaagctgccctgacctggc ccacctcgttacgacctaacatatggcgtgagtgcttcagccgctaccggatcatatgaagcaacacgactt cttaagtacgcatgcccgaaggctacgtccaggagcgaccatcttctcaaggacgacggcaactacaagac ccgcccggaggtgaagttcgagggcgacacctggtgaaccgcatcgagctgaagggcatcgacttcaaggagg acggcaacatcctggggcacaagctggagtacaactacaacagccacaacgtctatatcatggccgacaagcag aagaacggcatcaaggtgaacttcaagatccgccacaacatcgaggacggcagcgtgagctcggcaccacta ccagcagaacacccccatcggcgacggccccgtgctgctgcccgacaaccactacctgagcaccagtcggcct gagcaaagaccccaacgagaagcgcgatcacatggtcctgctggagtctgtgaccgcccgggatcactctcg catggacgagctgtacaagtaaaagcttctctcatgtaatgcatgctgctgctgctgcccgacaaccactac ctgagcaccagtcggccttggtttgtttttgttttttccgggtgctgttaaaaagaaagtcattctgtgttactgtagctt gtttgc ccatttc

Tet1 wt-3xF-T2A-tdTomato	gcagaccgggagtgctctgatgtatccccgaagccaatttatcacaccaaattccttctcgagttgcatcaacctt aaccgagacaatgttgtaccgtgtccccatactctctcactcatgttgccggaccatacaatcgttgggtcgact acaaagaccatgacgggtgattataaagatcatgatatcgattacaaggatgacgatgacaagggaagcgggagag ggcagaggaagtctgctaacatgcggtgacgtcgaggagaatcctggacctgtttccaaaggggaggaagtcatt aaggaatttatgaggtcaaagtgcgcatggaggatctatgaacggccacgaatttgagatagaaggcgaagg cgagggaaaggccctacgagggcactcagactgctaagctgaaagtaactaagggtgctctgcctttcgctg ggatatcctgtcaccagtttatgtacggtagtaaagcttatgtgaagcatcccgtgatatactgactataaaa aactgtccttccagagggctcaagtgggagcgagtaatgaacttgaagatggtggactggttaccgttacc agattcatctttgaggacgggaacattgatctacaaggtaagatgccccgactaactcccaccgacggggc agtcatgcagaagaagactatgggctgggaagctagtagcactctaccctagagatggtgtcttgaagg ggagattcatcaagcactgaaattgaaagacggcggtcattacctcgtcgaattcaaacatatacatggccaa aaagcctgtgcaactgccagggtattattatgtcgacacaaaactcgatataaccagccataatgaagattatacc atagtcaacaatatgaacgctctgaaggacgacatcattgttcttgggacatgggactggatccacaggatccg gttctctggaacagcatctccgaagacaataatggccgtaataaaagaattcatgcatcaaaagtgagaat ggaaggaagtatgaatggtcacgagttgaaatcgagggagaaggagagggtcggccctatgagggtacacag acagctaagttgaaggttactaaggcgcccttcccttggctgggatattctctccccacaattcatgtacggg tccaaggcttacgtaaacatccgctgatataaccgattacaaaaactgtccttccccgaaggctttaaagg aaagggtgatgaatttcgaggacgggggattggtaactgtcacacaggattcctcttcaagatggaacactgat ttacaaggtaaaaatgagagggaccaacttccccctgatgggcccgtgatgcaaaaagaaacatgggctggg aagcatctaccgagagactttatcccaggacggcgcttctaaggagagattaccaagcttgaacttaagg atggaggtcactacctcgtggagttaagacaatatatggcaaaaaaccagtccaactccccggatactatta cgttgataccaaactggacataacttctcataacgaggactacactatagtgaacaatatgaacgctctgagggt cgacaccacctttcctgtatggaatggatgaactgtataagtagtaaaagcttctctcatgtaatgcatttgctaat gtgggtagtgaggatTTTTGTTGTTGTTGTTTCTTTGTTTTTTGTTTTTCCGGTGTGTTAAAAAGAAAGTCATT ctgttcttactgtagcttctgcccatttc
--------------------------	---

Tet1 D2018A-3xF-T2A-tdTomato	gcagaccgggagtgctctgatgtatccccgaagccaatttatcacaccaaattccttctcgagttgcatcaacctt aaccgagccaatggtgtaccgtgtccccatactctctactcatgttgcgggaccatacaatcgttgggtcgact aaaagaccatgacgggtgattataaagatcatgatatcgattacaaggatgacgatgacaagggaagcggagag ggcagaggaagtctgctaacatgcggtgacgtcgaggagaatcctggacctgtttccaaaggggaggaagtcatt aaggaatttatgaggttcaaagtgcgcatggagggatctatgaacggccacgaatttgagatagaaggcgaagg cgagggaaaggccctacgagggcactcagactgctaagctgaaagtaactaagggtgctctgcctttcgctg ggatatcctgtcaccagtttatgtacggtagtaaagcttatgtgaagcatcccgtgatatactgactataaaa aactgtccttccagagggctcaagtgggagcgagtaatgaacttgaagatggtggactggttaccgttacc agattcatctttgaggacgggaacattgatctacaaggtaagatgcggggcactaactcccaccgacggggc agtcatgcagaagaagactatgggctgggaagctagtagcactctaccctagagatggtgtcttgaagg ggagattcaagcactgaaattgaaagacggcggtcattacctcgtgaattcaaaacctatacatggccaa aaagcctgtgcaactgccagggtattattatgtcgacacaaaactcgatataaccagccataatgaagattacc atagtcaacaatatgaacgctctgaaggacgacatcattgttcttgggacatgggactggatccaaggatccg gttctctggaacagcatctccgaagacaataatggccgtaataaaagaattcatgcgattcaaagtgagaat ggaaggaagtatgaatggtcacgagttgaaatcgagggagaaggagagggtcggccctatgagggtacacag acagctaagttgaaggtactaaggcgcccttcccttcttgggatattctctccccacaattcatgtacggg tccaaggcttacgtaaacatccgctgatataaccgattacaaaaactgtccttccccgaaggctttaaagg aaagggtgatgaatttcgaggacgggggattggtaactgtcacacaggattcctcttcaagatggaacactgat ttacaaggtaaaaatgagagggaccaacttccccctgatgggcccgtgatgcaaaaagaaaccatgggctggg aagcatctaccgagagactttatcccaggacggcggttctaaggagagattaccaagcttgaacttaagg atggaggtcactacctcgtggagttaagacaatatatggcaaaaaaccagtccaactccccggatactatta cgttgataccaaactggacataacttctcataacgaggactacactatagtgaacaatatgaacgctctgagggt cgacaccacctttcctgtatggaatggatgaactgtataagtagtaaaagcttctctcatgtaatgcatttgctaat gtgggtagtgaggatTTTTGTTGTTGTTGTTTCTTTGTTTTTTGTTTTTCCGGTGTGTTAAAAAGAAAGTCATT ctgttgttactgtagcttgtttcggccatttc
------------------------------	--

1224